



# HHS Public Access

## Author manuscript

*Chem Eng J.* Author manuscript; available in PMC 2023 August 03.

Author Manuscript

Author Manuscript

Author Manuscript

Author Manuscript

Published in final edited form as:

*Chem Eng J.* 2021 August ; 417: 129133. doi:10.1016/j.cej.2021.129133.

## Sensors for detecting per- and polyfluoroalkyl substances (PFAS): A critical review of development challenges, current sensors, and commercialization obstacles

Ruth F. Menger<sup>a</sup>, Emily Funk<sup>b</sup>, Charles S. Henry<sup>a,b</sup>, Thomas Borch<sup>a,c</sup>

<sup>a</sup>Department of Chemistry, Colorado State University, 1872 Campus Delivery, Fort Collins, CO 80523, USA

<sup>b</sup>Department of Chemical and Biological Engineering, Colorado State University, 1370 Campus Delivery, Fort Collins, CO 80523, USA

<sup>c</sup>Department of Soil and Crop Sciences, Colorado State University, 1170 Campus Delivery, Fort Collins, CO 80523, USA

### Abstract

Per- and polyfluoroalkyl substances (PFAS) are a class of compounds that have become environmental contaminants of emerging concern. They are highly persistent, toxic, bioaccumulative, and ubiquitous which makes them important to detect to ensure environmental and human health. Multiple instrument-based methods exist for sensitive and selective detection of PFAS in a variety of matrices, but these methods suffer from expensive costs and the need for a laboratory and highly trained personnel. There is a big need for fast, inexpensive, robust, and portable methods to detect PFAS in the field. This would allow environmental laboratories and other agencies to perform more frequent testing to comply with regulations. In addition, the general public would benefit from a fast method to evaluate the drinking water in their homes for PFAS contamination. A PFAS sensor would provide almost real-time data on PFAS concentrations that can also provide actionable information for water quality managers and consumers around the planet. In this review, we discuss the sensors that have been developed up to this point for PFAS detection by their molecular detection mechanism as well as the goals that should be considered during sensor development. Future research needs and commercialization challenges are also highlighted.

### Keywords

PFOA; PFOS; Fluorosurfactant; Nanoparticle; Molecularly imprinted polymer; Water quality

---

#### Declaration of Competing Interest

The authors declare that they have no known competing financial interests or personal relationships that could have appeared to influence the work reported in this paper.

## 1. Introduction

Per- and polyfluoroalkyl substances (PFAS) are a class of compounds that have recently become an area of significant concern. Originating from a variety of materials like stain repellents, nonstick coatings, cleaning products, and aqueous film forming foams (AFFFs), PFAS are ubiquitous in environments all over the world, even in the Arctic [1], [2], [3]. They can be found in [drinking water](#), surface water, soils, wildlife, plants, the atmosphere, and human food sources as well [4], [5], [6], [7], [8], [9], [10], [11], [12], [13], [14], [15], [16], [17], [18]. The high strength of the C-F bond makes PFAS thermodynamically stable and also resistant to typical degradation pathways like biodegradation [19] and photolysis [20]. This inability to break down in the environment gave PFAS the moniker of “forever” chemicals. The highest PFAS concentrations have been recorded near [wastewater treatment plants](#), firefighter training areas, landfill sites, and industrial sites [21]. These sources drain into environmental waters and then our drinking water sources. Human exposure to these chemicals is of high concern because they also build up in the human body and have been linked to a variety of human health issues, including prostate and kidney cancer, thyroid disease, and diabetes [11], [22], [23], [24], [25]. Studies have suggested that the toxicity comes from PFAS acting as an agonist for peroxisome proliferator-activated receptor alpha (PPAR $\alpha$ ). The activation of PPAR $\alpha$  interferes with the proper transcription of many target genes, leading to cancer development and other diseases [26], [27], [28].

The United States Environmental Protection Agency (EPA) [29] has set a health advisory level of 70 ppt (70 ng L<sup>-1</sup>) for lifetime exposure of perfluorooctanesulfonic acid (PFOS) and perfluorooctanoic acid (PFOA). Despite this guideline (which is currently not legally regulated), drinking water levels of up to 3000 times the lifetime advisory level have been reported in Colorado, North Carolina, and other hotspots across the US [30], [31], [32]. It is estimated that 54–83% of the US population (179–272 million people) is exposed to PFOS and PFOA contamination in their drinking water [33].

Due to their widespread application and use, PFAS are continually released during production, product use, and disposal via point and [nonpoint sources](#) into the environment [34]. Over 95% of PFAS are released into the [aquatic environment](#). A small portion (<5%) do volatilize and enter the atmosphere. There are over 5000 CAS numbers that are classified under PFAS, and the identity of most of them is unknown [35]. These unknown precursors can degrade into known PFAS [36]. PFOS and PFOA (Fig. 1) have been studied the most since they have been manufactured the longest [37], [38]. The U.S. EPA lifetime health advisory level was determined based on exposure studies of these two PFAS [39]. However, with so many other compounds that also contribute to the overall PFAS occurrence, the analysis of such a large class of compounds is challenging. PFAS range from short-chain fluorinated alkyl acids to long-chain compounds with a variety of functional groups. They can be cationic, anionic, or zwitterionic as well as linear, branched, or cyclic. PFAS can also be divided into groups by their head groups: perfluorocarboxylic acids (PFCAs) and perfluorosulfonic acids (PFSAs) [18], [40]. Manufacturers are starting to phase out long-chain PFAS ( C8 PFCAs and C6 PFSAs) in favor of short-chain PFAS ( C7 PFCAs, C5 PFSAs) that were thought to be less bio-accumulative and less toxic, like GenX (hexafluoropropylene oxide dimer acid, HFPO-DA). However, ongoing studies are showing

that GenX, 6:2 FTOH, and other short-chain PFAS may be just as toxic as their long-chain alternatives [11], [41], [42]. Some of the most common PFAS are shown in Fig. 1. As we begin to understand more about the global distribution of PFAS and replacement PFAS chemicals such as GenX and how toxic they can be, it is important to have a fast and cost-effective way to detect PFAS. In the past year, a few other reviews about PFAS sensors have been published that provide a broad overview of some alternative ways to detect PFAS [36], [43], [44], [45]. In contrast to these excellent papers, we present the recent progress in engineering sensors for PFAS from a molecular chemical perspective. Specifically, we present a brief overview of the current methods available for PFAS detection and their pitfalls, the challenges associated with the sensor development and the goals that should be kept in mind, and finally the sensors that have been developed up to this point. We discuss the detection mechanism of each sensor in detail to inform the reader how the sensor detects PFAS at a molecular level and also to establish what has already been tried and evaluated. As PFAS sensors are a very timely and relevant topic, we aim for this review to serve as a guide to establish the state of the field and to inspire further technological developments.

## 2. Current methods

Many laboratory-based techniques have been developed to detect PFAS using traditional analytical instruments [21], [36], [46], [47], [48], [49], [50]. The EPA currently has three approved methods for PFAS analysis: Methods 533, 537, and 537.1 [51], [52], [53]. These methods call for a polystyrene-divinylbenzene (SDVB) solid-phase extraction (SPE) step to concentrate the sample, followed by analysis with an LC-MS/MS fitted with a C18 column. Method 537.1 reports limits of detection (LOD) ranging 0.71–2.8 ppt for the 18 analytes while Method 533 reports lowest concentration minimum reporting limits of 1.4–16 ppt for 25 analytes [52], [53]. All three methods are sensitive and can analyze a combined total of 29 PFAS compounds but they are limited to [drinking water](#) samples and have a minimum 35 min LC-MS/MS run time. As of time of submission, the EPA is working on validation to include other matrices like surface water, groundwater, wastewater, soil, sediment, and [sludge](#) [54].

Other methods exist for the analysis of multiple PFAS in a variety of matrices, as recently reviewed by Al Amin et al., although these methods have not been validated by the U.S. EPA [36]. For example, variations of liquid chromatography coupled with mass spectrometry offer targeted analysis with sensitive quantitative determination in aqueous matrices, including drinking water [51], [55], groundwater [56], [57], [58], surface water [59], [60], river water [61], seawater [16], and wastewater [57], [62]. Ion chromatography [63], [64], [65] and fluorometric detection [66] can also provide LODs comparable to MS, but these methods require extensive pretreatment and/or derivatization with a fluorophore prior to analysis. Gas chromatography can only detect volatile, semi-volatile, and neutral PFAS which makes it less popular than LC [35], [36], [46] and the limits of detection are dependent on the detector. Capillary electrophoresis is portable but has poor detection limits (2–33 ppm) [67], [68].

Untargeted analysis can help quantify the total concentration of PFAS. It is difficult to quantify each of the 5000+ potentially relevant PFAS because standards don't exist

Author Manuscript

Author Manuscript

Author Manuscript

Author Manuscript

for all the compounds, so these methods aim to quantify PFAS as a compound class. The total oxidizable precursor assay (TOP) transforms PFAS precursors to dead-end perfluoroalkyl acids by a hydroxyl radical-based oxidation reaction to help determine the total concentration of PFAS present. The oxidized samples are still analyzed by HPLC-MS [69], [70]. Total organic [fluorine](#) (TOF) and total fluorine (TF, organic and inorganic) can be measured by particle-induced gamma ray emission (PIGE) [71], [72], combustion ion chromatography [48], [64], and fluorine-19 nuclear magnetic resonance (<sup>19</sup>F NMR) [73].

While the instrumental methods are effective at the right time and place, they are limited by high instrument cost and the requirement of a laboratory with trained personnel to run them. Costs of \$300-\$600 per sample are prohibitive in routine monitoring and do not allow for widespread sampling and testing of common PFAS [74]. To properly evaluate human risk of PFAS exposure, a simpler, faster, less expensive, and ideally field-based method is needed. Sensors, or devices that respond to an analyte and transform the chemical information into an analytically useful signal, have the potential to meet this demand for PFAS monitoring [75]. While PFAS exist in many matrices and detection therein is important, the detection of PFAS in aqueous matrices is a good first step to evaluate the risk of human exposure and the distribution of PFAS. Routine monitoring of these sources would allow more frequent testing of water samples to comply with regulations, providing actionable data to water quality managers. A fast detection method can help identify critical areas of PFAS contamination where remediation efforts should be focused [43]. Without the need for a central laboratory, the general public could potentially test their own drinking water using a fast and inexpensive test. A sensor for PFAS would not replace the traditional analytical techniques like LC-MS and GC-MS but instead complement their analysis by being able to provide fast and actionable data [43].

### 3. Challenges in sensor development

Sensor-based approaches for PFAS detection and analysis offer the potential for fast, on-site detection to evaluate water sources for PFAS exposure, but this comes with many challenges: (i) sensitivity, (ii) [selectivity](#), (iii) sample preparation and preconcentration, and (iv) portability. Before elaborating on these challenges, a brief discussion of the physical and chemical properties of PFAS is necessary. The C-F bond is very strong (485 kJ mol<sup>-1</sup>), which contributes to the thermodynamic stability of PFAS. The low polarizability of F also leads to weak intermolecular interactions like Van de Waals interactions and hydrogen bonding [76]. The C-F tail is hydrophobic while the sulfonic or [carboxylic acid](#) headgroups are hydrophilic. At high concentrations (greater than 1000 ppm), PFAS can form [micelles](#) and hemimicelles although in groundwater, these aggregations can occur at much lower concentrations due to interactions with particles and/or co-contaminants [77], [78]. Usually, PFAS are found as negatively charged anions, but depending on pH and other functional groups, cations and [zwitterions](#) also exist which can affect transportation and [sorption](#) [17]. These varied [physicochemical properties](#) make PFAS difficult to detect as a class.

First, sensors for PFAS detection need to have low limits of detection to be in accordance with the current guidelines. The U.S. EPA lifetime health advisory limit is currently set at 70 ppt for PFOS and PFOA, but many states and countries are moving to lower that limit as

[toxicology](#) studies indicate that even lower concentrations have negative health impacts [39], [79]. A 2012 study on immunotoxicity in children recommended a drinking water level of 1 ppt for PFOS and PFOA [80], [81]. Achieving such low limits of detection is challenging due to the complex nature of PFAS. There is often little to no interaction of the analyte with the electrode/probe/target at the molecular level and diffusion times are slow, contributing to high LODs [82], [83]. Additionally, due to the wide variety of PFAS compounds, sensitivity and selectivity suffer from the lack of specific receptors [84]. Solid-phase or liquid–liquid extraction methods can aid in preconcentrating a sample, but this adds additional steps to the analysis, limiting fast, field-based detection of PFAS [51], [85], [86], [87].

It is challenging to develop one sensor that is selective towards all the many different PFAS structures since they span a variety of chain lengths and head groups. A sensor can be designed to detect either PFCAs or PFSAs by focusing on the carboxylic or [sulfonic acid](#) head groups, for example, but there can be interferences from other PFAS and non-fluorinated surfactants, like sodium dodecyl sulfate (SDS) and sodium dodecylbenzenesulfonate (SDBS), depending on the detection mechanism. While a fully comprehensive sensor that can identify and quantify all PFAS would be ideal, a sensor that can detect and differentiate between PFOS and PFOA is a good start. Even so, there are still interferences from the hundreds to thousands of other PFAS present in environmental samples that need to be accounted for during sensor development. As short-chain PFAS like GenX become more prevalent, sensors for the new compounds in addition to the common existing PFAS will become necessary.

PFAS are prevalent in aqueous matrices including drinking water, groundwater, surface water (rivers and lakes), seawater, and wastewater, among many others [22]. Drinking water is a relatively clean matrix, having already been processed and treated, but environmental samples are not. Common components of environmental samples that can interfere with PFAS analysis include organic and inorganic ions, humic and fulvic acids, organic matter, and other surfactants [88], [89], [90], [91], [92], [93], [94]. For example, the structures of SDS and SDBS are similar to PFAS and can produce a similar response (PFOS, SDS, and SDBS all contain sulfonic acid functional groups). Solid-phase extraction (SPE) is common to both concentrate a sample and remove interfering ions and surfactants [56], [58], [60], [86]. However, this requires samples to be transported back to the lab, increasing total analysis time and cost, as well as increasing the risk of contamination to the sample [95]. Sample [pretreatment](#) and preconcentration consume 50–90% of the analysis time and labor costs [96]. Eliminating these steps or integrating them into a single step with the analysis is critical for a successful rapid screening procedure. The ability to use the sensor in a variety of matrices will help with identifying the sources of PFAS contamination as well as tracking downstream transport.

For a rapid screening procedure, a test that is portable and provides fast results is ideal. Both portable instruments and test kits offer this capability. Some of the previously mentioned instrument-based methods can use portable instruments that are small and light enough to be carried to and used at on-site testing areas [97], [98], [99]. There are still concerns regarding sensitivity, the need for trained personnel to use those instruments, and the cost of the instrument. Test kits offer a promising alternative that can be used by anyone. These

test kits manipulate capillary action to transport sample through a membrane, like paper or Nafion, into a detection region without external instrumentation. Pretreatment steps can be integrated into the device or kit, and detection is colorimetric or electrochemical. While they are inexpensive to manufacture and have low sample reagent requirements, they are single-use and only provide semi-quantitative results which can vary from person to person [100], [101]. For accurate readings, smartphones are becoming more common, using the high-resolution camera and a custom application to analyze images of the test and compare them against a built-in calibration curve [100], [102]. Other features like **GPS**, internet connection to upload results, as well as online help for on-site assistance, make smartphones a promising option for fast, portable sensors [103].

These challenges are all aspects to consider when developing a sensor or assay for fast detection of PFAS as part of a rapid screening procedure. Here we present the current state of sensors and assays for PFAS detection grouped by detection mechanism. We follow the IUPAC definition of sensor: “a device that transforms chemical information, ranging from the concentration of a specific sample component to total composition analysis, into an analytically useful signal” [75]. The sensors are summarized in the tables that follow each subsection.

## 4. Sensor-based methods

### 4.1. Small molecule complexation and assays

One of the simplest methods of detecting the presence of an analyte is with an organic dye that complexes with the analyte of interest and produces a visible color change. These dyes bind through different mechanisms such as NH-based hydrogen bonding, Lewis acid-base pairing, metal-ion-template, and transition metal complexing [103], [104], [105], [106]. The EPA has developed a method to detect surfactants, or methylene blue active substances (MBAS), in drinking water, surface water, and domestic and **industrial wastewaters** [107]. Methylene blue (MB), a cationic dye, is added to the sample and forms an ion-pair with the **anionic surfactant** which is then extracted into **chloroform**. The intensity of the blue color in the extract is proportional to the surfactant concentration and can be measured by UV–VIS over a range of 0.025–100 ppm [107], [108]. A variation of this method exists where an imidazolium derivative is immobilized on an inorganic solid support [109]. The anionic surfactant sample self-assembles into a monolayer with the hydrophobic alkyl chains pointing towards the bulk solution. When MB is added, it is trapped in the monolayer, turning the solution from colorless to blue proportional to the surfactant concentration with a limit of detection of 1 ppm. This method would be best for longer chain surfactants (>C10), as C6 and C8 linear alkyl chains did not respond well. While both methods are for general anionic surfactants, they could be used to detect PFAS as long as a pretreatment step is incorporated to eliminate the interference of SDS and SDBS, two common non-fluorinated anionic surfactants found in environmental water samples [110], [111].

Fang et al. [112] have developed a portable test kit for the colorimetric complexation of anionic surfactants with a cationic dye. The astkCARE kit uses ethyl violet (EV) instead of methylene blue and ethyl acetate instead of chloroform [113]. Similar to the MBAS assay, the cationic ethyl violet forms an immiscible ion pair with PFAS, and the color can be

measured after extraction into ethyl acetate. Since visual assessment of color is subjective, a smartphone app is available to read the color of the extracted EV-surfactant solution. A calibration step is also incorporated to determine the concentration of the unknown sample (Fig. 2A) [114]. An LOD of 10 ppb was reported without preconcentration. To eliminate interferences like inorganic ions and concentrate the sample, SPE or dual liquid–liquid extraction was performed, lowering the limit of detection to 0.5 ppb for PFOA and PFOS in spiked tap and groundwater [112]. Currently, the test is not specific for PFAS or even PFOS/PFOA as ethyl violet will form an ion-pair with any anionic surfactant. The same group has also developed a fluoro-SPE method that uses a fluoro-gel to separate PFAS from non-fluorinated anionic surfactants [115]. Pretreating a sample with SDVB-SPE and then fluoro-SPE makes it possible to more selectively detect PFAS with the test kit without interference from other surfactants but an LOD was not reported. The astkCARE kit is currently in early stages of [commercialization](#) and is being used across Royal Australian Air Force defense bases; however, the LOD (0.5 ppb) is still relatively high to evaluate drinking water [114].

Fluorescence detection is more sensitive than [colorimetry](#) and has been used for the detection of a variety of analytes [116], [117], [118], [119]. In 2015, Liang et al. [120] developed a sensing method that utilizes the ‘switch-on’ fluorescence of an eosin Y-polyethyleneimine-PFOS system. When polyethyleneimine (PEI) complexes with eosin Y, the fluorescence of the xanthene-based eosin Y dye is quenched. Once PFOS is added to the system, the PEI dissociates from the complex and the resulting turned-on fluorescence of the eosin Y-PFOS complex can be detected using a spectrofluorometer. The method has a limit of detection for PFOS of 7.5 ppb. One important thing to note is this assay is selective for PFOS: the lower [hydrophobicity](#) of PFOA prevents it from reacting with the eosin Y-PEI complex, resulting in very low fluorescence intensity. Other PFAS were not evaluated. A similar method by Cheng et al. [121] utilized ‘switch-on’ fluorescence with erythrosin B and cetyl trimethyl ammonium bromide (CTAB). The CTAB quenches the fluorescence emission of erythrosin B, but when PFOS or PFOA is added, mixed [micelles](#) are formed between CTAB and PFOS/PFOA, and the fluorescence intensity increases. This method is highly selective towards PFOS and PFOA: PFPrA, PFBA, PFPeA, PFHeA, PFHpA, PFDeA, PFBS, PFO, HFB, SDS, and SDBS were tested without significant interference. The sensor has limits of detection of 6.4 and 4.9 ppb for PFOS and PFOA, respectively, as well as a wide linear range (20.7–5001.3 ppb for PFOS, 20.7–4140.7 ppb for PFOA). Analogs of PFOS and PFOA, as well as other potentially co-existing substances like inorganic ions, were tested for interference with little change in fluorescence intensity, demonstrating [selectivity](#) for PFOS and PFOA. A lower LOD (0.5 ppb) was recently achieved by He et al. [122], where the fluorescence of a green fluorescent dye (trisodium-8-hydroypyrene-1,3,6-trisulfonate, HPTS) is quenched by protonated chitosan. PFOS binds to chitosan via electrostatic and hydrophobic interactions, restoring the fluorescence of HPTS (Fig. 3A). No other PFAS were evaluated. There was some interference from SDS and SDBS, but this can be removed by the addition of  $\text{Ba}^{2+}$  followed by filtration.

Another fluorescence-based method uses an indicator displacement assay with guanidinocalix[5]arene (GC5A) to detect PFOS and PFOA [123]. Fluorescein is reversibly bound to the GC5A receptor and is displaced by PFOS/PFOA, causing a linear increase in

fluorescence. Magnetic **iron oxide** nanoparticles were also bound to GC5A which enables the removal and concentration of the PFOS/PFOA complex with a magnet (LOD = ~10 ppb). This provides a large advantage over the other fluorescence detection methods; however, even with high removal efficiency (PFOS:  $99.57\% \pm 0.07$ , PFOA:  $98.47\% \pm 0.04$ ), the LOD is still not low enough to detect PFOS below the EPA drinking water standards. The fluorescence of the GC5A:PFOS/PFOA complex can also be measured with a smartphone and compared to a calibration curve to determine the concentration of an unknown (Fig. 2B), but an LOD for this method was not reported. Although other PFAS analogs were not tested, this method is likely specific for PFOS and PFOA due to the size of the cavity in GC5A.

A study was conducted by Fang et al. [124] which used aggregation-induced emission luminogens (AIEgen) to detect PFOA with a limit of detection of 41 ppb. A small droplet (1–2  $\mu\text{L}$ ) of AIEgen complexed with PFOA in an acetone–water solution is dropped into a hole in a glass slide. As the solution dries and the **acetone** evaporates, a micelle of PFOA forms and the AIEgen aggregates, inducing fluorescence which is proportional to the PFOA concentration. The method is not selective for PFOA, as PFOS and 6:2FTS showed similar results. The glass chip has the potential to be reused by washing thoroughly but the study did not examine this idea. If the chip is reusable, the cost efficiency of this detection method could be greatly improved.

Resonance light scattering (RLS) is related to fluorescence and specifically measures the intensity of the scattered excitation light. The electronic polarizability of the scattering particles will change the **light intensity** which allows RLS to be used as a detection method [125]. When PFAS complex with a dye or aggregate, the polarizability of the complex changes, allowing analyte detection. RLS has been used to detect PFOA and PFOS when they complex with cationic dyes by electrostatic attraction [90], [126], [127]. Qiao [126] and Zhang [90] reported the complexation of PFOS and PFOA, respectively, with crystal violet. The crystal violet-PFAS complex self-aggregates into nanoparticles, enhancing the **resonance scattering** intensities. The method developed by Qiao et al. improved the limit of detection (3 ppb) slightly by using triple-wavelength overlapping resonance Rayleigh scattering (TWO-RRS) where the intensity of three peaks at different wavelengths increased with the complexation of crystal violet and PFOS [126]. The method is stable across a wide pH range (5.0–11.0) but the change in RRS intensity gradually decreases as the ionic strength of the solution increases. More than 20 coexisting substances like vitamins, sugars, amino acids, and some metal ions were tested with little interference in PFOS detection. A benefit of this method is that measurement is very fast (<1 min), but this does not consider any sample preparation steps like potentially SPE and/or preconcentration. PFAS analogs will complex with a cationic dye like crystal violet, allowing this method to be used for quantification of total PFAS concentration. As non-fluorinated anionic surfactants are also likely to complex with cationic dyes, such interferences would need to be removed in a pretreatment step.

An even lower LOD was reported by Cheng et al. [127], using Janus Green B (JGB) to complex with PFOS (2.8 ppb). Other PFAS (PFOA, PFPrA, PFBA, PFPeA, PFHeA, PFHpA, PFNA, and PFBS) were evaluated as interferences, but they showed little RLS

Author Manuscript

Author Manuscript

Author Manuscript

Author Manuscript

response with JGB. The authors did not discuss a mechanism for how JGB is specific to PFOS over the other PFAS. SDS and SDBS did have considerable interference which can be eliminated by the addition of  $\text{Ba}^{2+}$ . Other potentially co-existing cations can be removed by cation exchange resin [90], [120], [127]. While the limits of detection reported by these RLS methods are still high compared to EPA guidelines, SPE and/or the addition of  $\text{Ba}^{2+}$  could be used as a pretreatment step to eliminate interferences and also preconcentrate the sample.

Chen et al. [128] combined three techniques for the [sensitive detection](#) of PFOS. This assay uses Nile blue A as a probe with fluorescence, RLS, and UV-Vis absorption detection (Fig. 3B). The sulfonic group of PFOS electrostatically interacts with the positively charged [nitrogen atoms](#) of Nile blue A, resulting in fluorescence quenching and decreased absorption intensity. The electrostatic interaction also causes ion association complexes to form hydrophobic interfaces with water molecules, resulting in enhanced RLS intensity. The lowest limit of detection found amongst the three [optical sensors](#) was 1.6 ppb from fluorescence. The assay was demonstrated with spiked tap and river water with a relative standard deviation of  $<2.14\%$ . This study showed the three-signal assay performs better than a single signal because of the ability to enhance the accuracy for the target analyte. This is especially relevant when developing a sensor to detect PFAS under EPA guidelines. In addition, the method is selective for PFOS, as there was not a significant difference in fluorescence intensity with or without other PFAS (PFOA, PFNA, PFHpA, PFHeA, PFBA, PFPeA, PFPtA, PFDeA).

While these small molecule complexation-based methods offer simple analyte detection, they often suffer from specificity and sensitivity concerns. The complexation molecules can often bind with multiple PFAS or even non-fluorinated surfactants. In addition, the limits of detection of these sensors are in the ppb range which is still too high for direct use in the field (Table 1). However, with benefits of few user steps and detection by smartphone, these sensors could be promising for on-site PFAS detection if a pretreatment step to lower the detection limits is built in.

## 4.2. Nanoparticles

Nanoparticle-based sensors have received much attention over the past few years due to benefits of sensitivity and selectivity at the nanoscale as well as ease of modification for a variety of applications, including environmental monitoring [103], [130], [131], [132], [133]. Gold nanoparticles (AuNP) in particular have been used for many years due to their unique optical, chemical, electrical, and catalytic properties [134]. Colorimetric detection of AuNP is driven by their aggregation and dispersion, and functionalizing the AuNP makes them selective towards the intended analyte [84]. Many reviews have been written about AuNP, different fabrication methods, applications, and detection methods [134], [135], [136], [137], [138], [139], [140], [141]. Fang et al. [103] specifically reviewed AuNP-based optical sensors for anionic contaminants, including PFOS and PFOA. In these sensors, AuNP were functionalized with thiol-terminated polystyrene or monolayers of alkanethiolates terminated with poly(ethylene glycol) (PEG-thiol) and perfluorinated thiols (F-thiol) [84], [89]. In the former sensor, PFOA displaces the polystyrene by binding to the AuNP, causing the AuNP to aggregate via F-F interactions and change the color from red

Author Manuscript

Author Manuscript

Author Manuscript

Author Manuscript

to blue-purple (Fig. 4A). The color change can be detected by the naked eye but not below 103 ppm, which is relatively high. The authors suggest that PFCAs as a group could also cause color-changing aggregation. In the latter sensor, the F-thiol allows for the binding of PFAS by F-F interactions, causing precipitation of the AuNP out of solution. As PFAS concentration increases, the red color of the solution decreases. The color change can be observed and measured by both naked eye and UV–Vis. Because of the general absorption of PFAS by the F-F interaction, multiple PFAS can be detected, but short-chain PFAS (<C7) have decreased sensitivity due to decreased hydrophobicity. Levels as low as 10 ppb could be detected for long-chain PFAS (>C7).

Colorimetric detection of PFOS has also been demonstrated with  $\text{Fe}_3\text{O}_4$  nanoparticles covalently bonded to  $\text{MoS}_2$ , an analog of graphene [142].  $\text{Fe}_3\text{O}_4$  NPs have peroxidase-like activity and can oxidize 3,3,5,5-tetramethylbenzidine (TMB) in the presence of  $\text{H}_2\text{O}_2$ , producing a blue color. When PFOS is present, the sulfonate head groups bind to the protonated hydroxyl groups on the surface of the  $\text{Fe}_3\text{O}_4$  NPs via electrostatic interactions and hydrogen bonding, inhibiting the peroxidase-like activity (Fig. 4B). The blue color change was detected with a [microplate](#) reader with an LOD of 4.3 ppb. PFOA also interacts with the  $\text{Fe}_3\text{O}_4$  NPs but less than PFOS, likely due to the difference between the carboxyl and sulfate headgroups. This method could potentially be used to detect total PFAS concentration, although mixtures of multiple PFAS would need to be tested as well. SDS and SDBS, which contain [sulfate groups](#), were shown to have considerable interference. Although not tested, it would be expected that sulfate anions would also interfere, but these interferences can likely be eliminated by SPE. The magnetic properties of the  $\text{Fe}_3\text{O}_4$  NPs could also be used to concentrate the sample, reducing the limit of detection.

Quantum dots (QD) are light-emitting semiconductor [nanomaterials](#) with [emission spectra](#) that can be tuned with the size of the QD and high fluorescent yield [143], [144]. Compared to organic dyes like the ones that were mentioned previously, QDs are brighter and have higher stability against photo and [chemical degradation](#) [143]. [Cadmium sulfide](#) quantum dots (CdS QDs) have been used to detect PFOA [145]. MPA (3-mercaptopropionic acid) stabilizes the CdS QDs and makes them hydrophilic, enabling aqueous samples to be analyzed. When PFOA is added to a solution of CdS QDs, the QDs aggregate via fluorine-fluorine affinity, inducing a change in fluorescence intensity (Fig. 4C). The limit of detection for this method is 124.2 ppb for PFOA and has a wide detection range of 207.03 ppb–16.56 ppm which could be useful in areas with high levels of contamination even though the LOD is not low enough to detect PFOA at the EPA guideline level. It was found that other PFCAs (C3–C7) could also quench the fluorescence of the QD but less than the effect from PFOA. Other carboxylic acids were also tested, with no significant quenching effect. Because the detection of PFOA with the CdS QDs is based on fluorine-fluorine interactions, PFOS and other PFASs could induce fluorescence quenching of the QDs as well but this was not evaluated.

Quantum dots synthesized out of carbon, called carbon dots (CDs) have advantages of lower cytotoxicity, simple synthesis, and low cost [146], [147]. Cheng et al. [148] synthesized blue fluorescent CDs whose fluorescence is quenched by complexation with berberine chloride hydrate (BH). When PFOS is added, the fluorescence is restored, likely due to

the electrostatic interaction of positively charged BH and PFOS, and the resulting change can be measured. The carbon dot-BH complex was tested in spiked water samples and proved successful for PFOS detection with a limit of detection of 10.8 ppb. A prominent feature of this method is that it can differentiate between PFOS and PFOA. PFOS is more hydrophobic and has greater electrostatic interaction with BH than PFOA, resulting in lower fluorescence intensity. Another CD for PFOS uses the measurement of three signals to detect PFOS [149]. The CDs are fabricated by hydrothermal synthesis with phosphoric acid and o-phenylenediamine (o-PD), resulting in pH-sensitive fluorescence emission (620 nm) at low pH values. When PFOS binds to the CDs, fluorescence is quenched, absorption is decreased, and resonance light scattering is enhanced. The fluorescence method of the assay is the most selective towards PFOS with a limit of detection of 9.1 ppb. Both of these methods tested other common PFAS (PFOA, PFDeA, PFPrA, PFBA, PFPeA, PFHeA, PFHpA, PFNA, PFBS) with little response, demonstrating selectivity for PFOS.

The emission of CDs can also be manipulated by doping the nanoparticles with other elements including nitrogen, boron, sulfur, or phosphorous [150]. Walekar [151] developed CDs doped with nitrogen and selenium in which the fluorescence of the CD is quenched by PFOA. The addition of PFOA appears to form an excited state complex and the fluorescence is quenched due to the internal transfer of electrons in the complex. The limit of detection for this method is 745.3 ppb but the surface of the carbon quantum dots could be further modified to optimize this method for lower limits of detection and other PFAS. Other PFCAs could potentially quench the fluorescence based on similar interaction with the CD, but PFNA had a smaller response compared to PFOA. PFOS had little effect on fluorescent quenching. Chen et al. [91] synthesized blue-green emissive nitrogen-doped carbon dots for ratiometric detection of PFOS. Ethidium bromide, which has an orange-red emission at the same excitation wavelength as the CDs, is added to the mixture of PFOS and CD and remains unchanged while PFOS quenches the CD fluorescence. The concentration of PFOS is determined by comparing the decrease in blue-green fluorescence to the unchanged orange-red peak. Using a fluorescence spectrophotometer, an LOD of 13.9 ppb was achieved. This method could also be optimized for visual analysis as the solution color changes from green to orange, which is more sensitive to the naked eye than a single color change. Unfortunately, both methods found that SDS and SDBS have high interferences so pretreatment must be implemented for samples [91], [149]. Other PFAS (PFOA, PFNA, PFHpA, PFHeA, PFBA, PFPeA, PFPrA, PFDeA) did not show significant interference.

Nanoparticle-based detection of other analytes has been incorporated into sensors like the home pregnancy test in a lateral flow assay format, demonstrating potential for these nanoparticle assays for PFAS to be made into a commercial product in a field-compatible format [152]. The intended use should be considered as some of these sensors would be beneficial for general PFAS detection while others would be useful for specific PFAS like PFOS or PFOA. Sensitivity requirements still need to be considered as these nanoparticle-based sensors have limits of detection in the ppb range (Table 2). However, there is room for improvement in optimizing the surface modifications to both lower limits of detection and also make the sensing motive more selective.

### 4.3. Molecularly imprinted polymers (MIP)

Molecularly imprinted polymers (MIP) have been very promising with respect to detecting PFAS. They have benefits of good sensitivity and selectivity in addition to being stable across a range of pH, temperature, and pressure values [130], [153], [154]. They can be reused without loss of activity. They are also relatively straightforward and inexpensive to synthesize with tunable surface properties and morphology [155]. Briefly, a MIP is prepared for a certain analyte by mixing the template molecule with functional [monomers](#), cross-linking monomers, and a radical initiator in a proper solvent. After polymerization and extraction of the template molecule, the cross-linked polymer forms a 3-dimensional cavity that can selectively rebind the original substrate molecule based on the electronic environment as well as the physical and chemical interactions between the cavity and the target molecule (Fig. 5A) [130]. They can also be functionalized using different moieties for a variety of detection techniques. For example, an electroactive functional monomer can be used to electrochemically detect the nonelectroactive PFAS with a MIP. Polypyrrole (Py) can serve as both the polymer matrix and the electron–ion transducer. Fang et al. [156] developed a MIP where Py is electrodeposited onto an inexpensive electrode surface, pencil lead, for potentiometric detection of PFOA. With potentiometric detection, an LOD of 441 ppb for PFOA was achieved. Chen et al. [157] also used the [electrodeposition](#) of Py as the polymer matrix for a MIP on ultrathin  $C_3N_4$  [nanosheets](#) as the electrode surface. Electrochemiluminescence was used as the detection method due to benefits of low cost, simple instrumentation, low background noise, and good stability against photobleaching. During the photolysis of coreactant  $S_2O_8^{2-}$ , powerful oxidants of sulfate radicals ( $SO_4^{2-}$ ) are generated which cause the oxidation of PFOA and a reduction in ECL signal. The authors report a detection limit of 10 ppt, which is one of the lowest presented in this review and comparable to traditional LC/MS methods [51], [52].

An electrochemical probe like ferrocenecarboxylic acid (FcCOOH) can also be added as a separate component for MIP-based detection of PFOS. A MIP was fabricated by the [electropolymerization](#) of o-phenylenediamine (o-PD) on a “classic” flat gold electrode [158], a [glassy carbon](#) macroelectrode [159], or a gold screen-printed electrode [160] respectively. O-PD is commonly used for MIP preparation because it can easily be electrodeposited to various substrates to form hydrophilic, hydrophobic, ionic, and acid-base recognition sites [158], [161]. FcCOOH acts as a reversible redox probe that produces an electrochemical signal at the electrode surface. When it competes for binding with PFOS, the voltammetric signal decreases. The glass carbon macroelectrode has an LOD of 25 ppt [159] while the classic gold electrode has an LOD of 20 ppt [158]. While screen printed electrodes are promising detection platforms due to their low cost, disposability, and portability, the authors reported poor performance by differential pulse voltammetry and difficulties in reproducibility [160].

Without the addition of a chemical probe, [photoelectrochemistry](#) can also be used to detect PFAS, as demonstrated by Tran [162] and Gong [163]. In this detection method, light induces the [electron transfer](#) process at the electrode surface. Tran et al. developed a MIP using acrylamide, ethylene glycol dimethylacrylate (EGDMA), and azobisisobutyronitrile (AIBN) as the functional monomer, crosslinker, and initiator agent, respectively, on a  $TiO_2$

Author Manuscript

Author Manuscript

Author Manuscript

Author Manuscript

nanotube array, which is a great photochemical **semiconductor material** [164], [165]. The **photocurrent** increases in the presence of increasing PFOS concentrations. The authors reported an LOD for PFOS of 86 ppb [162]. Another MIP based on the same polymerization reagents anchors the MIP on an AgI nanoparticle-BiOI nanoflake array [163]. This array has the advantage of facile synthesis as well as enhanced performance for photochemical applications. MIPs on nanoparticles have a high surface area:volume ratio, which increases accessibility to the imprinted cavities as well as increasing binding kinetics [130], [166], which was previously mentioned as a challenge in achieving low limits of detection. The mechanism of the nanoflake array is slightly different compared to the MIP@TiO<sub>2</sub>: in this case, photocurrent decreases as PFOA concentration increases [163]. The presence of PFOA in the MIP sterically blocks the diffusion of the electron donor triethanolamine (TEA) to the sensing surface and the oxidation of TEA does not occur, decreasing the photocurrent signal. This sensor has an LOD of 0.01 ppb, which is comparable to or even lower than traditional instrument-based methods [36].

Fluorescence and **photoluminescence** can also be used as detection mechanisms with MIPs as demonstrated by Feng et al. [167] and Zheng et al. [168]. In both cases, a MIP was synthesized of 3-aminopropyltriethoxysilane (APTES, functional monomer) and tetraethoxysilane (TEOS, cross-linker). The fluorescence MIP was anchored on the surface of SiO<sub>2</sub> nanoparticles (NP) onto which a hybrid monolayer was formed of a fluorescein dye (FITC) and organic amine ligands [167]. When PFOS binds to the amine ligands in the MIP cavities, the electron transfer from the fluorescence dye to the PFOS results in quenched fluorescence. With detection by a fluorescence spectrophotometer, an LOD of 5.57 ppb for PFOS was reported. The photoluminescence MIP was anchored on a CdTe@CdS core–shell quantum dot (Fig. 5B) [168]. In the presence of PFOA, photoluminescence is quenched. The interference of PFOS, SDS, and SDBS was evaluated and found to be less effective in quenching the photoluminescence of the quantum dots because they cannot fit in the cavity as effectively. The authors report an LOD of 10.35 ppb and good reproducibility in spiked river samples.

In another variation of a MIP – nanoparticle combination, a chitosan-based MIP was doped with fluorescent carbon dots [169]. In the presence of PFOS, the fluorescence emission of the CD increases. The authors calculated the LOD to be 0.0004 ppt without preconcentration, which is the lowest LOD of all methods evaluated in this review, but no concentrations below 0.02 ppt were evaluated. Such low concentrations should be ideally be verified by LC/MS but the validated LC/MS methods have higher LODs at 1.4–16 ppt [51], [52]. The MIP-nanoparticle method was demonstrated in biological samples (serum and urine) as well. With proper optimization in environmental samples and more testing at lower PFOS concentrations, this method could be very promising for low concentration PFOS detection.

A benefit of MIPs is that they are selective for the analyte used as the template molecule to make the MIP film. The detection of the analyte depends on the compatibility between the cavity and the analyte molecule in terms of size, charge, and chemistry. For example, Chen et al. [157] demonstrated little response of a PFOA-MIP to analogs of PFOA with similarity in structures, like PFOS, PCP, 2,4-D, MP, PFPrA, PFBA, PFHxA, PFHpA, PFNA,

PFDeA). Karimian [158] found that smaller analogs than the target molecule can easily access the MIP binding sites, but the interference effects from the smaller molecules did not affect detection of PFOS, demonstrating higher affinity of the MIP for PFOS. Kazemi et al. [159] sought to develop an analytically rigorous method to quantify the effects from interferences so they evaluated PFOA and PFBS at multiple concentrations in a PFOS MIP electrode and determined  $K_A$  values from a Langmuir isotherm binding model. They found that PFOA and PFBS have comparable  $K_A$  values to PFOS, demonstrating that multiple PFAS could be detected with their PFOS MIP on a glass carbon macroelectrode. The high selectivity for a single molecule would be ideal for a sensor for a single PFAS. However, to detect and quantify total PFAS concentration, a mixed MIP or even multiple MIPs for all the different PFAS would be very challenging since so many of the molecules are unknown and/or standards to make the MIP do not exist.

For the detection of GenX (i.e., HFPO-DA), one of the new generation PFAS molecules, Glasscott et al. have successfully fabricated a MIP on a gold microelectrode which is currently the only sensor available that is selective for GenX [172]. With a template of o-PD on a gold microelectrode, the presence of GenX in the MIP cavity reduces the surface area available for the oxidation of ferrocene methanol which serves as the redox probe. The authors determined a limit of detection of 0.086 ppt, which is well below a provisional limit of 140 ppt which has been set by the North Carolina Department of Health and Human Services [170]. The MIP-microelectrode was also selective for GenX in the presence of NaCl, [humic acid](#), or PFOS. During the detection of GenX in river water, the authors found that matrix effects of polymer swelling may impact the performance of the MIP as indicated by different limits of quantification between river water and ammonium buffer. This point should also be kept in mind when evaluating the other MIPs in environmental samples.

Sensors based on MIPs perform best for detecting specific PFAS. Some have also been able to achieve low enough LODs to make them promising for detecting PFAS below guideline levels (Table 3). After preparation of the MIP matrix, [leakage](#) can occur where the template has not been completely removed from the matrix, interfering with the accuracy of analyte detection [171].

#### 4.4. Optical fibers

Optical fibers offer the ability to be used in a variety of fields with many advantages. They can be directly connected to an online platform or even a smartphone and be used for continuous and remote monitoring of pollutants [173], [174], [175]. Additionally, the fibers are flexible with large fiber diameters, can easily be optimized, handled and installed, and involve low-cost, simple manufacturing [176], [177], [178]. The most common detection method with optical fibers is [surface plasmon resonance](#), where an analyte is detected based on a change in resonance wavelength when the analyte interacts with ligands on a metallic surface layer on the optical fiber (Table 4) [179], [180]. Typically the fibers are silica-based, but Cennamo et al. from the Zeni group have developed a low-cost optical fiber made of plastic (POF) that is easier and less expensive to manufacture [176], [181]. The fiber is D-shaped and coated in a buffer layer (Microposit S1813) before sputtering a gold film and depositing a MIP layer which detects the PFAS (Fig. 6A) [174], [182], [183], [184]. The

MIP for PFOA was prepared using PFOA as the template, (vinylbenzyl)trimethylammonium chloride (VBT) and 1H,1H,2H,2H-perfluorodecyl acrylate (PFDA) as the functional monomers, EGDMA as the cross-linker, and AIBN as the radical initiator [184]. After 10 min incubation with an aqueous sample, the change in resonance wavelength was detected by a [spectrometer](#) with an LOD of 130 ppt for PFOA. A mixture of 11 PFAS (C4-C11) was detected with an LOD of 150 ppt [182]; however, this goes against what other MIP-based methods found where PFAS that were not the template molecule were not able to be detected.

A halogen light and spectrometer setup is not the most accessible for detection so a low-cost detection setup has been developed as well using LED lights, two photodetectors, and a digital low-cost [oscilloscope](#) connected to a laptop to detect the intensity change through the same MIP-POF platform. With an LOD of 500 ppt for PFOA, this offers a lower cost and slightly more portable alternative to a spectrometer but at the disadvantage of a higher limit of detection [183]. The same group has also presented another alternative by replacing the oscilloscope and laptop with an Arduino system connected to a Raspberry Pi for automatic data acquisition and processing, leading to continuous [water monitoring](#) [174].

Cennamo et al. [177] have also used the surface plasmon resonance optical fiber as a [biosensor](#), using an antibody to bind PFOA. The same POF with a Microposit buffer layer and gold film was used, but instead of a MIP as the receptor layer, a monospecific anti-PFOA antibody was covalently immobilized to the gold chip by an amide crosslinker. After 10 min room temperature incubation with the sample, the resonance wavelength was recorded with a limit of detection of 240 ppt for PFOA in buffer. A sample with high ionic strength to mimic seawater was also tested, resulting in an LOD of 880 ppt. PFOS was also evaluated with a similar response to PFOA, but a mixed solution was not tested nor were other PFAS.

The previous POF sensors have the sensor component in the middle of the fiber. Another optical fiber for PFOA was recently developed by Faiz et al. [185]. In this work, they formed a [polyvinylidene](#) fluoride (PVDF) coating on the end of a cleaved optical fiber using an immersion precipitation-based phase inversion process. When PFOA adsorbs to the surface of the PVDF membrane at the end of the fiber due to electrostatic and hydrophobic interactions, the apparent thickness of the coating changes, resulting in a change in the optical path difference (Fig. 6B). This fiber had a limit of detection of 5 ppm. While they did test the fiber successfully with samples of diluted AFFF containing potentially multiple PFAS, the limit of detection is still relatively high, and no interferences were tested. With appropriate optimization and evaluation of selectivity for certain PFAS or PFAS mixtures, optical fibers offer a promising approach for remote and continuous sensing/monitoring of PFAS.

#### 4.5. Immunosensors

[Immunoassays](#) offer an interesting approach to PFAS detection. These sensors take inspiration from how PFAS act in the human body. For example, PFOS and PFOA bind strongly to both bovine and human serum albumin (hSA) [186], [187], [188], [189]. Moro et al. [190] developed an electrochemical sensor based on hSA covalently immobilized

Author Manuscript

Author Manuscript

Author Manuscript

Author Manuscript

to pyrrole-2-carboxylic acid (Py-2-COOH) on a graphite screen-printed electrode. In this immunoassay, the hSA was delipidated to increase the binding sites for PFOA [186]. The impedance of the sensor increases when PFOA binds to the hSA. PFOS does increase the impedance signal but PFOS was not evaluated at multiple concentrations. This immunosensor is promising in that it is label-free, robust, fast, and disposable due to the use of the screen-printed electrode, but it still needs to be developed past proof of concept and fully evaluated as a standalone sensor for interferences, selectivity, and sensitivity, as well as use in real samples [190] (Table 5).

PFAS have been recognized as an agonist for peroxisome proliferator-activated receptor alpha (PPAR $\alpha$ ), which is a transcription factor that activates many target genes [26], [27]. The activation of PPAR $\alpha$  by PFOS has been associated with cancer development and other diseases [28]. The activated complex can be captured by monoclonal anti-PPAR $\alpha$  antibodies on a microplate [191], [192]. In one immunosensor, AuNPs modified with PPAR $\alpha$ -responsive elements (PPRE) are added to the microplate and bind only to the activated complex (Fig. 7A). Silver was also added to enhance the signal of the AuNP. The **optical density** positively corresponds to the PFOS concentration, with a limit of detection of 5 ppt. As other molecules that can activate PPAR $\alpha$ , PFOA and mono(2-ethylhexyl) phthalate (MEHP) were also quantified [191]. In another sensor, quantum dots modified with streptavidin serve as a fluorescent marker that bind to the PFOS-activated PPAR $\alpha$  complex (Fig. 7B) [192]. The fluorescence intensity of the quantum dots is proportional to the PFOS concentration, with an LOD of 2.5 ppt. While neither of these PPAR $\alpha$  sensors are field-compatible as they require many reagent addition, washing, and incubation steps which can take hours, a microplate enables the analysis of 96 samples at once. Still, the concept is promising and could be adapted to a lateral flow assay format for on-site detection of total PFAS concentration.

Enzymatic biosensors for PFOS have also been developed. Multi-walled carbon nanohorn-modified glassy carbon electrodes act as the bioanode and biocathode substrates [193]. Glutamic **dehydrogenase** and bilirubin **oxidase** are the biocatalysts that convert chemical energy into electrical energy when L-glutamate is oxidized in the presence of NAD $^+$ . PFOS inhibits the activity of the biocatalysts and decreases the voltage of the system. This change in open-circuit voltage was measured by cyclic voltammetry, and the limit of detection was found to be 800 ppt. The biosensor is selective for PFOS as PFOA, PFBS salt, PFOSA, and PFNA did not have any interference.

#### 4.6. Other

A type of material that is more commonly being used in sensors is organic frameworks: metal and covalent. Both are **porous materials** that can be tuned to be selective to allow certain molecules into their pores. Metal organic frameworks (MOFs) are made of rigid inorganic groups and flexible organic linker ligands. Extremely high surface area and pore volume allow multiple binding sites that help address low detection limit concerns [194]. Specifically with electrochemical detection, MOFs can be used directly on electrodes as electrode extensions as demonstrated by the Chatterjee group [195]. The MOF, with a Cr metal center, traps PFOS by strong electronic affinity. An interdigitated microelectrode array

was used as an electrochemical transducer to make **impedance measurements**. The use of the array increased the signal-to-noise ratio compared to a conventional macro electrode. An LOD of 0.5 ppt was obtained, which is one of the lowest of the methods discussed in this review. Although no other PFAS were tested with the MOF, the sensor was able to detect spiked PFOS in untreated groundwater which is promising for its use in realistic matrices.

Covalent organic frameworks (COFs) are similar to MOFs but are composed of light elements like hydrogen, carbon, boron, nitrogen, and oxygen which form **covalent bonds** in a cyclic manner [196]. Li et al. [197] functionalized **lanthanide** upconversion nanoparticles (UCNPs) with COFs to detect PFOS. In the presence of PFOS, the fluorescence of the UCNPs@COFs allows for highly sensitive detection using a fluorescence spectrometer. PFHxS, PFDA, PFNA, PFOA, PFHpA, and PFHxA also quench the fluorescence of the NP but not as much as PFOS. Interfering effects from SDS and SDBS could be eliminated by the addition of  $\text{Ba}^{2+}$ . The limit of detection (0.075 ppt) achieved by this sensor is extremely low in comparison to other fluorescence detection methods and well below the current EPA guideline of allowable PFOS in drinking water.

Ion-selective electrodes (ISE) have also been developed for *in situ* PFOS/PFOA detection by manipulating F-F interactions and transducing the chemical signal into an electrical signal. A fluorophilic methyltriarylpophosphonium cation membrane has been shown to be highly selective for  $\text{PFO}^-$  and  $\text{PFOS}^-$  with limits of detection in the low ppb range [198], [199].

## 5. Commercialization

While significant progress has been made towards PFAS sensors, commercialization has lagged. Of all the sensors presented in this review, we are aware of only one in early stages of commercialization [112], [114] and two others with submitted patent applications [158], [195], [200], [201]. In order to progress the field beyond the research setting and impact how PFAS are measured in the field, one must consider the technology transfer process and commercialization early in the development cycle. **Commercialization** is an important activity as a mechanism to provide sensors to end users that are interested in the information that is provided by the sensors more than how they work. Sensors for both environmental and toxicological applications are envisioned based on the need to understand where there is PFAS pollution and how widely it **impacts humans**. For environmental applications, sensors can support tracing and detection to protect human and ecological health. Sensors will also be critical once guidelines are in place as a way to reduce analysis cost and time. Sensors are not meant to replace the traditional instrumental methods that are currently being used, but instead complement their analysis and make the detection of PFAS more accessible. Commercializing PFAS sensors has proven challenging for several reasons. First, the performance requirements (detection limits, matrices, etc.) are challenging for any sensor necessitating longer development cycles. As a result, it can be expensive to develop the sensors in large quantities while maintaining the necessary performance level. Second, until recently the demand (market pull) has been limited, placing further challenges on the economics of production.

Despite these challenges, there is hope for future commercialized PFAS sensors. First, the U.S. EPA proposed regulatory determinations for PFOS and PFOA under the Safe Drinking Water Act in February 2020 [54]. Previously PFOS and PFOA have been monitored but not regulated. This proposal follows similar regulatory efforts passed in the EU in 2019 [202]. Given the high cost of traditional PFAS analysis methods, sensors that can provide relevant, cost-effective information will be valuable to water management systems. Second, the performance of traditional sensors using, like ion-selective electrodes, has improved to the point that they can provide useful information while also being a form factor that makes production viable based on existing platforms once suitable modifications have been made for PFAS detection. Even with this progress, however, there is a clear need to continue progress towards commercializing sensors that can provide useful, actionable information for water quality managers.

## 6. Summary and outlook

This review summarizes the latest developments in sensor-based detection of PFAS by discussing the various detection mechanisms. There is still a lot of research and optimization to be done as these sensors have pitfalls including high limits of detection, long analysis time, and/or still need a pretreatment step to reduce the impact of interferences. The key for detection is to find something that will capture PFAS and transduce the binding event into a measurable analytical signal. In addition to the detection methods described above, we can draw inspiration from the work done to clean up water sources. For example, activated carbon, anion exchange membranes, and [nanofiltration](#) have been used to remove PFAS from wastewater [203]. Other removal and adsorption techniques that have been developed but not evaluated as a sensor for detection include fluorinated gel [204], [cyclodextrins](#) [155], [205], [206], [207], [208], MIPs [95], [206], [209], [210], [211], [212], and MOFs [213]. These methods could be used to capture the PFAS from an environmental sample and then be combined with a signal transduction step for detection.

A big point that was made evident was the difference between a sensor that is specific for one PFAS compound (like PFOS or PFOA) or a sensor that can detect PFCAs, PFSAs, or total PFAS. While both types are useful, the purpose of the sensor should be kept in mind. To evaluate water sources for their compliance with EPA guidelines, a sensor that is specific to PFOS and/or PFOA is important as the current guidelines are for total PFOA and PFOS content (70 ppt). This type of sensor could be used by both water quality managers and the general public. Of the sensors described above, those with MIPs had the best response to a specific PFAS without interference from other PFAS. For general PFAS detection, sensors based on complexation with organic dyes and nanoparticles as well as PPAR $\alpha$  immunosensors performed best. These [optical sensors](#), especially those based on small molecule complexation, also tend to suffer from interferences like other surfactants like SDS and SDBS which will need to be removed prior to PFAS detection. As more studies are done and other PFAS are regulated, it will become important to detect the other common PFAS like the ones included in the EPA standard methods [51], [52], [53]. So far, only one sensor has been developed for GenX, part of the next generation of short-chain PFAS [172]. As the chemistry of these compounds is different from PFOS, PFOA, and other long-chain PFAS, new detection mechanisms may need to be developed.

Many of the sensors that we described test real samples in the form of tap, river, and/or lake water. However, in most cases, the PFAS concentration was too low to be detected so the samples were spiked with PFAS to demonstrate [feasibility](#). Further optimization and testing need to be done to demonstrate the use of the sensors in real matrices out in the field. A big part of this is to continue lowering the limits of detection of the sensor to the low ppt range and below. This can be done by optimizing pretreatment and preconcentration steps although adding extra steps is not ideal for field-based measurements. The development of fluoro-SPE is promising as a further step to make a sensor more specific for PFAS [115]. In the meantime, sensors with detection limits in the high ppt to low ppb range can still perform well as a prescreening tool to identify hotspots of PFAS contamination in aqueous environmental samples.

Currently, the sensors with the lowest LODs (<25 ppt) are either a MIP electrode [157], [158], [159], [163], [172] or an [immunoassay](#) [191], [192]. All of these have instrumentation needs like a potentiostat or a [microplate](#) reader, neither of which are field-compatible in their traditional form. Again, the end user should be kept in mind. A water quality lab with the ability to accommodate some infrastructure like a potentiostat or a microplate reader would benefit from the MIP and immunosensors, but this set up would not provide the general public with an inexpensive and easy-to-use sensor. Two sensors mentioned previously use a smartphone to read the results of a colorimetric reaction of PFAS with ethyl violet or guanidinocalix[5]arene [112], [123]. While the LODs of these sensors are still relatively high (~10 ppb), the use of a smartphone is a promising step towards a field-compatible quantitative sensor. Smartphones also have the ability to integrate into a network of smart sensing technology, increasing our ability to map and monitor PFAS contamination [44].

As research and development of these sensors continue, the process towards commercialization should also be kept in mind, including making the sensor in a form factor that is conducive to its intended purpose. While the publication of the method is often the end of the line within academia, many industries including government agencies, water quality managers, and contract labs as well as the general public will benefit from taking the extra steps to bring a sensor to the commercial market. The widespread use of a PFAS sensor can make a big difference in how we study and treat PFAS in addition to ensuring human and environmental health.

## Acknowledgments

The authors acknowledge the High Plains Intermountain Center for Agricultural Health and Safety (CDC NIOSH U54OH008085) for financially supporting this work.

## Nomenclature

<b>2,4-D</b>	2,4-dichlorophenoxyacetic acid
<b>6:2 FTS</b>	6:2 fluorotelomer sulfonate
<b>8:2F FTOH</b>	8:2 fluorotelomer alcohol
<b>FFF</b>	aqueous film forming foam

<b>AIBN</b>	azobisisobutyronitrile
<b>AIegen</b>	aggregation-induced emission luminogens
<b>APTES</b>	3-aminopropyltriethoxysilane
<b>AuNP</b>	gold nanoparticle
<b>BH</b>	berberine chloride hydrate
<b>CD</b>	carbon dot
<b>COF</b>	covalent organic framework
<b>CTAB</b>	cetyl trimethyl ammonium bromide
<b>EGDMA</b>	ethylene glycol dimethylacrylate
<b>EPA</b>	Environmental Protection Agency
<b>EV</b>	ethyl violet
<b>FcCOOH</b>	ferrocenecarboxylic acid
<b>FITC</b>	fluorescein isothiocyanate
<b>GC5A</b>	guanidinocalix[5]arene
<b>GenX</b>	2,3,3,3-tetrafluoro-2-(heptafluoropropoxy)propanoic acid
<b>GPS</b>	global position system
<b>HFB</b>	heptafluoro-1-butanol
<b>HFPO-DA</b>	hexafluoropropylene oxide-dimer acid
<b>HPLC</b>	high performance liquid chromatography
<b>HPTS</b>	trisodium-8-hydroypyrene-1,3,6-trisulfonate
<b>hSA</b>	human serum albumin
<b>IC</b>	ion chromatography
<b>ISE</b>	ion-selective electrode
<b>IUPAC</b>	International Union of Pure and Applied Chemistry
<b>JGB</b>	Janus Green B
<b>LC-MS/MS</b>	liquid chromatography tandem mass spectrometry
<b>LOD</b>	limit of detection
<b>MB</b>	methylene blue
<b>MBAS</b>	methylene blue active substances

<b>MEHP</b>	mono(2-ethylhexyl) phthalate
<b>MIP</b>	molecularly imprinted polymer
<b>MOF</b>	metal organic framework
<b>MP</b>	methyl parathion
<b>MPA</b>	3-mercaptopropionic acid
<b>NAD<sup>+</sup></b>	nicotinamide adenine dinucleotide
<b>NMR</b>	nuclear magnetic resonance
<b>NP</b>	nanoparticle
<b>OF</b>	optical fiber
<b>o-PD</b>	o-phenylenediamine
<b>PCP</b>	pentachlorophenol
<b>PEI</b>	polyethyleneimine
<b>PFAS</b>	per- and polyfluoroalkyl substances
<b>PFBA</b>	perfluorobutanoic acid
<b>PFBS</b>	perfluorobutanesulfonic acid
<b>PFBSK</b>	nonafluorobutanesulfonic acid potassium
<b>PFCA</b>	perfluorocarboxylic acid
<b>PFDA</b>	1H,1H,2H,2H-perfluorodecyl acrylate
<b>PFDeA</b>	perfluorodecanoic acid
<b>PFHeA</b>	perfluorohexanoic acid
<b>PFHpA</b>	perfluoroheptanoic acid
<b>PFHxA</b>	perfluorohexanoic acid
<b>PFHxS</b>	perfluorohexanesulfonic acid
<b>PFNA</b>	perfluorononanoic acid
<b>PFO</b>	perfluorooctane
<b>PFOA</b>	perfluorooctanoic acid
<b>PFOS</b>	perfluorooctanesulfonic acid
<b>PFOSA</b>	perfluorooctanesulfonamide
<b>PFPeA</b>	perfluoropentanoic acid

<b>PFPrA</b>	perfluoropropionic acid
<b>PFSA</b>	perfluorosulfonic acid
<b>PIGE</b>	particle-induced gamma ray emission
<b>POF</b>	plastic optical fiber
<b>PPAR<math>\alpha</math></b>	peroxisome proliferator-activated receptor alpha
<b>PPRE</b>	PPAR $\alpha$ -responsive elements
<b>Py</b>	polypyrrole
<b>Py-2-COOH</b>	pyrrole-2-carboxylic acid
<b>QD</b>	quantum dot
<b>RLS</b>	resonance light scattering
<b>SDBS</b>	sodium dodecylbenzenesulfonate
<b>SDS</b>	sodium dodecyl sulfate
<b>SDVB</b>	poly(styrene–divinylbenzene)
<b>SPE</b>	solid-phase extraction
<b>TEA</b>	triethanolamine
<b>TEOS</b>	tetraethoxysilane
<b>TWO-RRS</b>	triple-wavelength overlapping resonance Rayleigh scattering
<b>UCNP</b>	upconversion nanoparticles
<b>UV-Vis</b>	ultraviolet – visible spectroscopy
<b>VBT</b>	(vinylbenzyl)trimethylammonium chloride

## References

- [1]. Butt CM, Berger U, Bossi R, Tomy GT Levels and trends of poly- and perfluorinated compounds in the arctic environment *Sci. Total Environ.*, 408 (2010), pp. 2936–2965 [PubMed: 20493516]
- [2]. Yamashita N, Taniyasu S, Petrick G, Wei S, Gamo T, Lam PKS, Kannan K Perfluorinated acids as novel chemical tracers of global circulation of ocean waters *Chemosphere*, 70 (2008), pp. 1247–1255 [PubMed: 17854858]
- [3]. Ross I, McDonough J, Miles J, Storch P, Thelakkat Kochunarayanan P, Kalve E, Hurst J, Dasgupta SS, Burdick J A review of emerging technologies for remediation of PFASs *Remediation*, 28 (2018), pp. 101–126
- [4]. Benskin JP, Li B, Ikonomou MG, Grace JR, Li LY Per- and Polyfluoroalkyl Substances in Landfill Leachate: Patterns, Time Trends, and Sources *Environ. Sci. Technol.*, 46 (2012), pp. 11532–11540 [PubMed: 23030600]
- [5]. Domingo JL, Nadal M Per-and polyfluoroalkyl substances (PFASs) in food and human dietary intake: a review of the recent scientific literature *J. Agric. Food Chem.*, 65 (2017), pp. 533–543 [PubMed: 28052194]

[6]. Herzke D, Olsson E, Posner S Perfluoroalkyl and polyfluoroalkyl substances (PFASs) in consumer products in Norway - A pilot study *Chemosphere*, 88 (2012), pp. 980–987 [PubMed: 22483730]

[7]. Hu XC, Andrews DQ, Lindstrom AB, Bruton TA, Schaider LA, Grandjean P, Lohmann R, Carignan CC, Blum A, Balan SA, Higgins CP, Sunderland EM Detection of Poly- and Perfluoroalkyl Substances (PFASs) in U.S. Drinking Water Linked to Industrial Sites, Military Fire Training Areas, and Wastewater Treatment Plants *Environ. Sci. Technol. Lett.*, 3 (2016), pp. 344–350 [PubMed: 27752509]

[8]. Goosey E, Harrad S Perfluoroalkyl substances in UK indoor and outdoor air: Spatial and seasonal variation, and implications for human exposure *Environ. Int.*, 45 (2012), pp. 86–90 [PubMed: 22580294]

[9]. Loi EIH, Yeung LWY, Mabury SA, Lam PKS Detections of Commercial Fluorosurfactants in Hong Kong Marine Environment and Human Blood: A Pilot Study *Environ. Sci. Technol.*, 47 (2013), pp. 4677–4685 [PubMed: 23521376]

[10]. Smithwick M, Norstrom RJ, Mabury SA, Solomon K, Evans TJ, Stirling I, Taylor MK, Muir DCG Temporal Trends of Perfluoroalkyl Contaminants in Polar Bears (*Ursus maritimus*) from Two Locations in the North American Arctic, 1972–2002 *Environ. Sci. Technol.*, 40 (2006), pp. 1139–1143 [PubMed: 16572767]

[11]. Sunderland EM, Hu XC, Dassuncao C, Tokranov AK, Wagner CC, Allen JG A review of the pathways of human exposure to poly- and perfluoroalkyl substances (PFASs) and present understanding of health effects *J. Exposure Sci. Environ. Epidemiol.*, 29 (2019), pp. 131–147

[12]. Szostek B, Prickett KB Determination of 8:2 fluorotelomer alcohol in animal plasma and tissues by gas chromatography-mass spectrometry *J. Chromatogr. B*, 813 (2004), pp. 313–321

[13]. Van de Vijver KI, Hoff P, Das K, Brasseur S, Van Dongen W, Esmans E, Reijnders P, Blust R, De W Coen Tissue distribution of perfluorinated chemicals in harbor seals (*Phoca vitulina*) from the Dutch Wadden Sea *Environ. Sci. Technol.*, 39 (2005), pp. 6978–6984 [PubMed: 16201619]

[14]. Verreault J, Houde M, Gabrielsen GW, Berger U, Hauks M, Letcher RJ, Muir DCG Perfluorinated Alkyl Substances in Plasma, Liver, Brain, and Eggs of Glaucous Gulls (*Larus hyperboreus*) from the Norwegian Arctic *Environ. Sci. Technol.*, 39 (2005), pp. 7439–7445 [PubMed: 16245813]

[15]. Xiao X, Ulrich BA, Chen B, Higgins CP Sorption of Poly- and Perfluoroalkyl Substances (PFASs) Relevant to Aqueous Film-Forming Foam (AFFF)-Impacted Groundwater by Biochars and Activated Carbon *Environ. Sci. Technol.*, 51 (2017), pp. 6342–6351 [PubMed: 28582977]

[16]. Yamashita N, Kannan K, Taniyasu S, Horii Y, Okazawa T, Petrick G, Gamo T Analysis of perfluorinated acids at parts-per-quadrillion levels in seawater using liquid chromatography-tandem mass spectrometry *Environ. Sci. Technol.*, 38 (2004), pp. 5522–5528 [PubMed: 15575267]

[17]. Place BJ, Field JA Identification of Novel Fluorochemicals in Aqueous Film-Forming Foams Used by the US Military *Environ. Sci. Technol.*, 46 (2012), pp. 7120–7127 [PubMed: 22681548]

[18]. Backe W, Field JA Zwitterionic, cationic, and anionic fluorinated chemicals in aqueous film forming foam formulations and groundwater at US military bases by non-aqueous large volume injection HPLC-MS/MS *Environ. Sci. Technol.*, 47 (2013), pp. 5226–5234 [PubMed: 23590254]

[19]. Liou JSC, Szostek B, Derito CM, Madsen EL Investigating the biodegradability of perfluoroctanoic acid *Chemosphere*, 80 (2010), pp. 176–183 [PubMed: 20363490]

[20]. Vaalgamaa S, Vähätilo AV, Perkola N, Huhtala S Photochemical reactivity of perfluorooctanoic acid (PFOA) in conditions representing surface water *Sci. Total Environ.*, 409 (2011), pp. 3043–3048 [PubMed: 21592543]

[21]. Dauchy X Per- and polyfluoroalkyl substances (PFASs) in drinking water: Current state of the science *Curr. Opin. Environ. Sci. Health*, 7 (2019), pp. 8–12

[22]. Ahrens L, Bundschuh M Fate and effects of poly- and perfluoroalkyl substances in the aquatic environment: A review *Environ. Toxicol. Chem.*, 33 (2014), pp. 1921–1929 [PubMed: 24924660]

[23]. Butenhoff JL, Kennedy GL Jr., Frame SR, O'Connor JC, York RG The reproductive toxicology of ammonium perfluoroctanoate (APFO) in the rat *Toxicology*, 196 (2004), pp. 95–116 [PubMed: 15036760]

[24]. Hekster FM, Laane RWPM, De Voogt P Environmental and Toxicity Effects of Perfluoroalkylated Substances Rev. Environ. Contam. Toxicol, 179 (2003), pp. 99–121 [PubMed: 15366585]

[25]. Kudo N, Kawashima Y Toxicity and toxicokinetics of perfluorooctanoic acid in humans and animals J. Toxicol. Sci, 28 (2003), pp. 49–57 [PubMed: 12820537]

[26]. Hurst CH, Waxman DJ Activation of PPAR and PPAR by Environmental Phthalate Monoesters Toxicol. Sci, 74 (2003), pp. 297–308 [PubMed: 12805656]

[27]. Shipley JM trans-Activation of PPAR and Induction of PPAR Target Genes by Perfluorooctane-Based Chemicals Toxicol. Sci, 80 (2004), pp. 151–160 [PubMed: 15071170]

[28]. Klaunig JE, Babich MA, Baetcke KP, Cook JC, Corton JC, David RM, DeLuca JG, Lai DY, McKee RH, Peters JM PPAR $\alpha$  agonist-induced rodent tumors: modes of action and human relevance Crit. Rev. Toxicol, 33 (2003), pp. 655–780 [PubMed: 14727734]

[29]. Lifetime Health Advisories and Health Effects Support Documents for Perfluorooctanoic Acid and Perfluorooctane Sulfonate, U.S. Environmental Protection Agency, Washington, D.C., 2016.

[30]. Finley B Colorado ramps up response to toxic “forever chemicals” after discovery of hot spots across metro Denver Denver Post Denver, Colorado (2019)

[31]. White D Denver Post Article on Colorado Response to High Levels of PFAS Association of State Drinking Water Administrators (2019)

[32]. PFAS Contamination in the U.S. Environmental Working Group, 2020.

[33]. Andrews DQ, Naidenko OV Population-Wide Exposure to Per- and Polyfluoroalkyl Substances from Drinking Water in the United States Environ. Sci. Technol, Lett (2020)

[34]. Sharifan H, Bagheri M, Wang D, Burken JG, Higgins CP, Liang Y, Liu J, Schaefer CE, Blotevogel J Fate and transport of per- and polyfluoroalkyl substances (PFASs) in the vadose zone Sci. Total Environ, 145427 (2021)

[35]. Nakayama SF, Yoshikane M, Onoda Y, Nishihama Y, Iwai-Shimada M, Takagi M, Kobayashi Y, Isobe T Worldwide trends in tracing poly- and perfluoroalkyl substances (PFAS) in the environment, TrAC Trends Anal. Chem, 121 (2019), Article 115410

[36]. Al Amin M, Sobhani Z, Liu Y, Dharmaraja R, Chadalavada S, Naidu R, Chalker JM, Fang C Recent advances in the analysis of per- and polyfluoroalkyl substances (PFAS) - A review Environ. Technol. Inno, 19 (2020), Article 100879

[37]. Giesy JP, Kannan K Perfluorochemical surfactants in the environment Environ. Sci. Technol, 36 (2002), pp. 147–152

[38]. Giesy JP, Kannan K Global distribution of perfluorooctane sulfonate in wildlife Environ. Sci. Technol, 35 (2001), pp. 1339–1342 [PubMed: 11348064]

[39]. Cordner A, De La Rosa VY, Schaider LA, Rudel RA, Richter L, Brown P Guideline levels for PFOA and PFOS in drinking water: the role of scientific uncertainty, risk assessment decisions, and social factors J. Exposure Sci. Environ. Epidemiol, 29 (2019), pp. 157–171

[40]. Martin D, Munoz G, Mejia-Avendaño S, Duy SV, Yao Y, Volchek K, Brown CE, Liu J, Sauvé S Zwitterionic, cationic, and anionic perfluoroalkyl and polyfluoroalkyl substances integrated into total oxidizable precursor assay of contaminated groundwater Talanta, 195 (2019), pp. 533–542 [PubMed: 30625579]

[41]. Rice PA, Aungst J, Cooper J, Bandele O, Kabadi SV Comparative analysis of the toxicological databases for 6:2 fluorotelomer alcohol (6:2 FTOH) and perfluorohexanoic acid (PFHxA) Food and Chemical Toxicology, 138 (2020), Article 111210

[42]. Cannon RE, Richards AC, Trexler AW, Juberg CT, Sinha B, Knudsen GA, Birnbaum LS Effect of GenX on P-Glycoprotein, Breast Cancer Resistance Protein, and Multidrug Resistance-Associated Protein 2 at the Blood-Brain Barrier Environ Health Perspect, 128 (2020), Article 037002

[43]. Naidu R, Nadebaum P, Fang C, Cousins I, Pennel K, Conder J, Newell C, Longpré D, Warner S, Crosbie N Per-and poly-fluoroalkyl substances (PFAS) current status and research needs Environ. Technol. Inno (2020), Article 100915

[44]. Rodriguez KL, Hwang J-H, Esfahani AR, Sadmani AHMA, Lee WH Recent Developments of PFAS-Detecting Sensors and Future Direction: A Review Micromachines, 11 (2020), p. 667 [PubMed: 32650577]

[45]. Ryu H, Li B, De Guise S, McCutcheon J, Lei Y Recent progress in the detection of emerging contaminants PFASs *J. Hazard. Mater.*, 124437 (2020)

[46]. Trojanowicz M, Koc M Recent developments in methods for analysis of perfluorinated persistent pollutants *Microchim. Acta*, 180 (2013), pp. 957–971

[47]. Coggan TL, Anumol T, Pyke J, Shimeta J, Clarke BO A single analytical method for the determination of 53 legacy and emerging per- and polyfluoroalkyl substances (PFAS) in aqueous matrices *Anal. Bioanal. Chem.*, 411 (2019), pp. 3507–3520 [PubMed: 31073731]

[48]. McDonough CA, Guelfo JL, Higgins CP Measuring total PFASs in water: The tradeoff between selectivity and inclusivity *Curr. Opin. Environ. Sci. Health*, 7 (2019), pp. 13–18 [PubMed: 33103012]

[49]. Onghena M, Moliner-Martinez Y, Picó Y, Campíns-Falcó P, Barceló D Analysis of 18 perfluorinated compounds in river waters: Comparison of high performance liquid chromatography–tandem mass spectrometry, ultra-high-performance liquid chromatography–tandem mass spectrometry and capillary liquid chromatography–mass spectrometry *J. Chromatogr. A*, 1244 (2012), pp. 88–97 [PubMed: 22633866]

[50]. Pan Y, Wang J, Yeung LWY, Wei S, Dai J Analysis of emerging per- and polyfluoroalkyl substances: Progress and current issues, *TrAC Trends Anal. Chem.*, 124 (2020), Article 115481

[51]. Shoemaker JA, Grimmett PE, Boutin BK Method 537: Determination of Selected Per- and Polyfluorinated Alkyl Substances in Drinking Water by Solid Phase Extraction and Liquid Chromatography/Tandem Mass Spectrometry (LC/MS/MS) U.S. Environmental Protection Agency, Office of Research and Development, National Exposure Research Laboratory, Washington, D.C. (2018)

[52]. Shoemaker JA, Tettenhorst DR, Method 537.1: Determination of selected per- and polyfluorinated alkyl substances in drinking water by solid phase extraction and liquid chromatography/tandem mass spectrometry (LC/MS/MS), U.S. Environmental Protection Agency, Office of Research and Development, National Center for Environmental Assessment, Washington, D.C., 2020.

[53]. Rosenblum L, Wendelken SC Method 533: Determination of per- and polyfluoroalkyl substances in drinking water by isotope dilution anion exchange solid phase extraction and liquid chromatography/tandem mass spectrometry U.S. Environmental Protection Agency, Office of Ground Water and Drinking Water, Cincinnati, OH (2019)

[54]. EPA Pfas Action Plan Program Update U.S. Environmental Protection Agency, Washington, D.C. (2020)

[55]. Tröger R, Klöckner P, Ahrens L, Wiberg K Micropollutants in drinking water from source to tap - Method development and application of a multiresidue screening method *Sci. Total Environ.*, 627 (2018), pp. 1404–1432

[56]. Wei C, Wang Q, Song X, Chen X, Fan R, Ding D, Liu Y Distribution, source identification and health risk assessment of PFASs and two PFOS alternatives in groundwater from non-industrial areas *Ecotoxicol. Environ. Saf.*, 152 (2018), pp. 141–150 [PubMed: 29402442]

[57]. Field JA, Schultz M, Barofsky D Fluorinated alkyl surfactants in groundwater and wastewater *Chimia*, 57 (2003), pp. 22–34

[58]. Janda J, Nödler K, Brauch H-J, Zwiener C, Lange FT Robust trace analysis of polar (C2–C8) perfluorinated carboxylic acids by liquid chromatography-tandem mass spectrometry: method development and application to surface water, groundwater and drinking water *Environ. Sci. Pollut. Res.*, 26 (2018), pp. 7326–7336

[59]. Simcik MF, Dorweiler KJ Ratio of perfluorochemical concentrations as a tracer of atmospheric deposition to surface waters *Environ. Sci. Technol.*, 39 (2005), pp. 8678–8683 [PubMed: 16323762]

[60]. Dalahmeh S, Tigrani S, Komakech AJ, Niwagaba CB, Ahrens L Per- and polyfluoroalkyl substances (PFASs) in water, soil and plants in wetlands and agricultural areas in Kampala, Uganda *Sci. Total Environ.*, 631–632 (2018), pp. 660–667

[61]. Takino M, Daishima S, Nakahara T Determination of perfluorooctane sulfonate in river water by liquid chromatography/atmospheric pressure photoionization mass spectrometry by automated

on-line extraction using turbulent flow chromatography *Rapid Commun. Mass Spectrom.*, 17 (2003), pp. 383–390 [PubMed: 12590385]

[62]. Gallen C, Eaglesham G, Drage D, Nguyen TH, Mueller JF A mass estimate of perfluoroalkyl substance (PFAS) release from Australian wastewater treatment plants *Chemosphere*, 208 (2018), pp. 975–983 [PubMed: 30068041]

[63]. Hori H, Hayakawa E, Einaga H, Kutsuna S, Koike K, Ibusuki T, Kiatagawa H, Arakawa R Decomposition of environmentally persistent perfluoroctanoic acid in water by photochemical approaches *Environ. Sci. Technol.*, 38 (2004), pp. 6118–6124 [PubMed: 15573615]

[64]. Miyake Y, Yamashita N, Rostkowski P, So MK, Taniyasu S, Lam PK, Kannan K Determination of trace levels of total fluorine in water using combustion ion chromatography for fluorine: a mass balance approach to determine individual perfluorinated chemicals in water *J. Chromatogr. A*, 1143 (2007), pp. 98–104 [PubMed: 17229428]

[65]. Janda J, Nödler K, Scheurer M, Happel O, Nürenberg G, Zwiener C, Lange FT Closing the gap – inclusion of ultrashort-chain perfluoroalkyl carboxylic acids in the total oxidizable precursor (TOP) assay protocol *Environ. Sci. Process Impacts*, 21 (2019), pp. 1926–1935 [PubMed: 31183483]

[66]. Pobo y E, Król E, Wójcik L, Wachowicz M, Trojanowicz M HPLC determination of perfluorinated carboxylic acids with fluorescence detection *Microchim. Acta*, 172 (2011), pp. 409–417

[67]. Wójcik L, Korczak K, Szostek B, Trojanowicz M Separation determination of perfluorinated carboxylic acids using capillary zone electrophoresis with indirect photometric detection *J. Chromatogr. A*, 1128 (2006), pp. 290–297 [PubMed: 16837005]

[68]. Wójcik L, Szostek B, Maruszak W, Trojanowicz M Separation of perfluorocarboxylic acids using capillary electrophoresis with UV detection *Electrophoresis*, 26 (2005), pp. 1080–1088 [PubMed: 15765482]

[69]. Houtz EF, Sedlak DL Oxidative Conversion as a Means of Detecting Precursors to Perfluoroalkyl Acids in Urban Runoff *Environ. Sci. Technol.*, 46 (2012), pp. 9342–9349 [PubMed: 22900587]

[70]. Zhang C, Hopkins ZR, McCord J, Strynar MJ, Knappe DR Fate of Per-and Polyfluoroalkyl Ether Acids in the Total Oxidizable Precursor Assay and Implications for the Analysis of Impacted Water *Environ. Sci. Technol. Lett.*, 6 (2019), pp. 662–668 [PubMed: 31909080]

[71]. Schaider LA, Balan SA, Blum A, Andrews DQ, Strynar MJ, Dickinson ME, Lunderberg DM, Lang JR, Peaslee GF Fluorinated Compounds in U.S Fast Food Packaging, *Environ. Sci. Technol. Lett.*, 4 (2017), pp. 105–111 [PubMed: 30148183]

[72]. Ritter EE, Dickinson ME, Harron JP, Lunderberg DM, DeYoung PA, Robel AE, Field JA, Peaslee GF PIGE as a screening tool for Per-and polyfluorinated substances in papers and textiles *Nucl. Instrum. Methods Phys. Res., Sect. B*, 407 (2017), pp. 47–54

[73]. Moody CA, Kwan WC, Martin JW, Muir DC, Mabury SA Determination of perfluorinated surfactants in surface water samples by two independent analytical techniques: liquid chromatography/tandem mass spectrometry and 19F NMR *Anal. Chem.*, 73 (2001), pp. 2200–2206 [PubMed: 11393841]

[74]. Laboratory Testing, Department of Environment, Great Lakes, and Energy Michigan PFAS Action Response Team, Michigan, 2020.

[75]. Hulanicki A, Glab S, Ingman F Chemical Sensors Definitions and Classification *Pure Appl. Chem.*, 63 (1991), pp. 1247–1250

[76]. Kiss E Fluorinated surfactants and repellants (Second ed.), Marcel Dekker Inc, New York (2001)

[77]. Brusseau ML Assessing the potential contributions of additional retention processes to PFAS retardation in the subsurface *Sci. Total Environ.*, 613 (2018), pp. 176–185 [PubMed: 28915454]

[78]. Bhattacharai B, Gramatica P Prediction of Aqueous Solubility, Vapor Pressure and Critical Micelle Concentration for Aquatic Partitioning of Perfluorinated Chemicals *Environ. Sci. Technol.*, 45 (2011), pp. 8120–8128 [PubMed: 20958003]

[79]. Gobelius L, Hedlund J, Dürig W, Tröger R, Lilja K, Wiberg K, Ahrens L Per-and polyfluoroalkyl substances in Swedish groundwater and surface water: implications for environmental quality standards and drinking water guidelines *Environ. Sci. Technol.*, 52 (2018), pp. 4340–4349 [PubMed: 29527894]

[80]. Post GB, Cohn PD, Cooper KR Perfluorooctanoic acid (PFOA), an emerging drinking water contaminant: A critical review of recent literature *Environ. Res.*, 116 (2012), pp. 93–117 [PubMed: 22560884]

[81]. Grandjean P, Clapp R Perfluorinated alkyl substances: emerging insights into health risks *New Solut.*, 25 (2015), pp. 147–163 [PubMed: 26084549]

[82]. Baronas R, Kulys J, Lan inskas A, Žilinskas A Effect of Diffusion Limitations on Multianalyte Determination from Biased Biosensor Response Sensors, 14 (2014), pp. 4634–4656 [PubMed: 24608006]

[83]. Baronas R Nonlinear effects of diffusion limitations on the response and sensitivity of amperometric biosensors *Electrochim. Acta*, 240 (2017), pp. 399–407

[84]. Takayose M, Akamatsu K, Nawafune H, Murashima T, Matsui J Colorimetric detection of perfluorooctanoic acid (PFOA) utilizing polystyrene-modified gold nanoparticles *Anal. Lett.*, 45 (2012), pp. 2856–2864

[85]. Karrman A, van Bavel B, Jarnberg U, Hardell L, Lindstrom G Development of a solid-phase extraction-HPLC/single quadrupole MS method for quantification of perfluorochemicals in whole blood *Anal. Chem.*, 77 (2005), pp. 864–870 [PubMed: 15679355]

[86]. Van Leeuwen SPJ, De Boer J Extraction and clean-up strategies for the analysis of poly- and perfluoroalkyl substances in environmental and human matrices *J. Chromatogr. A*, 1153 (2007), pp. 172–185 [PubMed: 17349649]

[87]. He X, He Y, Huang S, Fang Z, Liu J, Ma M, Chen B Fluoro-functionalized paper-based solid-phase extraction for analysis of perfluorinated compounds by high-performance liquid chromatography coupled with electrospray ionization–tandem mass spectrometry *J. Chromatogr. A*, 1601 (2019), pp. 79–85 [PubMed: 31208796]

[88]. Jeon J, Kannan K, Lim BJ, An KG, Kim SD Effects of salinity and organic matter on the partitioning of perfluoroalkyl acid (PFAs) to clay particles *J. Environ. Monitor.*, 13 (2011), p. 1803

[89]. Niu H, Wang S, Zhou Z, Ma Y, Ma X, Cai Y Sensitive Colorimetric Visualization of Perfluorinated Compounds Using Poly(ethylene glycol) and Perfluorinated Thiols Modified Gold Nanoparticles *Anal. Chem.*, 86 (2014), pp. 4170–4177 [PubMed: 24684731]

[90]. Zhang F, Zheng Y, Liang J, Long S, Chen X, Tan K A simple and highly sensitive assay of perfluorooctanoic acid based on resonance light scattering technique *Spectrochim. Acta, Part A*, 159 (2016), pp. 7–12

[91]. Chen Q, Zhu P, Xiong J, Gao L, Tan K A new dual-recognition strategy for hybrid ratiometric and ratiometric sensing perfluorooctane sulfonic acid based on high fluorescent carbon dots with ethidium bromide *Spectrochim. Acta, Part A*, 224 (2020), Article 117362

[92]. Powley CR, George SW, Ryan TW, Buck RC Matrix Effect-Free Analytical Methods for Determination of Perfluorinated Carboxylic Acids in Environmental Matrixes *Anal. Chem.*, 77 (2005), pp. 6353–6358 [PubMed: 16194099]

[93]. Cheng J, Vecitis CD, Park H, Mader BT, Hoffmann MR Sonochemical Degradation of Perfluorooctane Sulfonate (PFOS) and Perfluorooctanoate (PFOA) in Landfill Groundwater: Environmental Matrix Effects *Environ. Sci. Technol.*, 42 (2008), pp. 8057–8063 [PubMed: 19031902]

[94]. Taniyasu S, Kannan K, So MK, Gulkowska A, Sinclair E, Okazawa T, Yamashita N Analysis of fluorotelomer alcohols, fluorotelomer acids, and short- and long-chain perfluorinated acids in water and biota *J. Chromatogr. A*, 1093 (2005), pp. 89–97 [PubMed: 16233874]

[95]. Cao F, Wang L, Ren X, Wu F, Sun H, Lu S The application of molecularly imprinted polymers in passive sampling for selective sampling perfluorooctanesulfonic acid and perfluorooctanoic acid in water environment *Environ. Sci. Pollut. Res.*, 25 (2018), pp. 33309–33321

[96]. Tang S, Zhang H, Lee HK Advances in Sample Extraction *Anal. Chem.*, 88 (2016), pp. 228–249 [PubMed: 26616153]

[97]. Foster SW, Xie X, Pham M, Peaden PA, Patil LM, Tolley LT, Farnsworth PB, Tolley HD, Lee ML, Grinias JP Portable capillary liquid chromatography for pharmaceutical and illicit drug analysis *J. Sep. Sci.*, 43 (2020), pp. 1623–1627 [PubMed: 31960568]

[98]. Liu B, Wu T, Yang X, Wang Z, Du Y Portable Microfluidic Chip Based Surface-Enhanced Raman Spectroscopy Sensor for Crystal Violet Anal. Lett, 47 (2014), pp. 2682–2690

[99]. Obeidat S, Bai B, Rayson GD, Erson DM, Puscheck AD, Landau SY, Glasser T A multi-source portable light emitting diode spectrofluorometer Appl. Spectrosc, 62 (2008), pp. 327–332 [PubMed: 18339242]

[100]. Morbioli GG, Mazzu-Nascimento T, Stockton AM, Carrilho E Technical aspects and challenges of colorimetric detection with microfluidic paper-based analytical devices ( $\mu$ PADs) - A review Anal. Chim. Acta, 970 (2017), pp. 1–22 [PubMed: 28433054]

[101]. Gong MM, Sinton D Turning the Page: Advancing Paper-Based Microfluidics for Broad Diagnostic Application Chem. Rev, 117 (2017), pp. 8447–8480 [PubMed: 28627178]

[102]. Ozer T, McMahon C, Henry CS Advances in Paper-Based Analytical Devices Annu. Rev. Anal. Chem, 13 (2020), pp. 85–109

[103]. Fang C, Dharmarajan R, Megharaj M, Naidu R Gold nanoparticle-based optical sensors for selected anionic contaminants, TrAC Trends Anal. Chem, 86 (2017), pp. 143–154

[104]. Santos-Figueroa LE, Moragues ME, Climent E, Agostini A, Martínez-Máñez R, Sancenón F Chromogenic and fluorogenic chemosensors and reagents for anions. A comprehensive review of the years 2010–2011 Chem. Soc. Rev, 42 (2013), p. 3489 [PubMed: 23400370]

[105]. Moragues ME, Martínez-Máñez R, Sancenón F Chromogenic and fluorogenic chemosensors and reagents for anions. A comprehensive review of the year Chem. Soc. Rev, 40 (2011) (2009), pp. 2593–2643 [PubMed: 21279197]

[106]. Duke RM, Veale EB, Pfeffer FM, Kruger PE, Gunnlaugsson T Colorimetric and fluorescent anion sensors: an overview of recent developments in the use of 1, 8-naphthalimide-based chemosensors Chem. Soc. Rev, 39 (2010), pp. 3936–3953 [PubMed: 20818454]

[107]. Method 425.1 Methylene Blue Active Substances (MBAS) Standard Methods for the Examination of Water and Wastewater American Public Health Association, Washington, DC, USA (1992)

[108]. Chitikela S, Dentel SK, Allen HE Modified method for the analysis of anionic surfactants as methylene blue active substances Analyst, 120 (1995), pp. 2001–2004

[109]. Coll C, Martínez-Máñez R, Marcos MD, Sancenón F, Soto J A Simple Approach for the Selective and Sensitive Colorimetric Detection of Anionic Surfactants in Water Angew. Chem. Int. Ed, 46 (2007), pp. 1675–1678

[110]. Field JA, Barber LB, Thurman EM, Moore BL, Lawrence DL, Peake DA Fate of Alkylbenzenesulfonates and Dialkyltetralinsulfonates in Sewage-Contaminated Groundwater Environ. Sci. Technol, 26 (1992), pp. 1140–1148

[111]. Chen Y, Wang S-Y, Wu R-F, Qi D-Y, Zhou T-Z Spectrophotometric determination of trace anionic surfactants such as SDS and SDBS in water after preconcentration on an organic solvent-soluble membrane filter Anal. Lett, 31 (1998), pp. 691–701

[112]. Fang C, Zhang X, Dong Z, Wang L, Megharaj M, Naidu R Smartphone app-based/portable sensor for the detection of fluoro-surfactant PFOA Chemosphere, 191 (2018), pp. 381–388 [PubMed: 29049961]

[113]. N. R Mallavarapu Megharaj, Mercurio P, USPTO Anionic surfactant detection CRC Care Pty Ltd (2013)

[114]. astkCARE: anionic surfactant detection, Cooperative Research Centre for Contamination Assessment and Remediation of the Environment, 2020.

[115]. Al Amin M, Sobhani Z, Chadalavada S, Naidu R, Fang C Smartphone-based / Fluoro-SPE for selective detection of PFAS at ppb level Environ. Technol. Inno, 18 (2020), Article 100778

[116]. Nguyen MP, Kelly SP, Wydallis JB, Henry CS Read-by-eye quantification of aluminum (III) in distance-based microfluidic paper-based analytical devices Anal. Chim. Acta, 1100 (2020), pp. 156–162 [PubMed: 31987136]

[117]. Rasheed T, Bilal M, Nabeel F, Iqbal HMN, Li C, Zhou Y Fluorescent sensor based models for the detection of environmentally-related toxic heavy metals Sci. Total Environ, 615 (2018), pp. 476–485

[118]. De Acha N, Elosúa C, Corres JM, Arregui FJ Fluorescent sensors for the detection of heavy metal ions in aqueous media Sensors, 19 (2019), p. 599 [PubMed: 30708989]

[119]. Lakowicz JR *Fluorescence Sensing* Lakowicz JR (Ed.), *Principles of Fluorescence Spectroscopy*, Springer, Boston, MA (2006), pp. 623–673

[120]. Liang J, Deng X, Tan K An eosin Y-based “turn-on” fluorescent sensor for detection of perfluoroctane sulfonate *Spectrochim. Acta, Part A*, 150 (2015), pp. 772–777

[121]. Cheng Z, Du L, Zhu P, Chen Q, Tan K An erythrosin B-based “turn on” fluorescent sensor for detecting perfluoroctane sulfonate and perfluoroctanoic acid in environmental water samples *Spectrochim. Acta, Part A*, 201 (2018), pp. 281–287

[122]. He J, Su Y, Sun Z, Zhang R, Wu F, Bai Y A chitosan-mediated “turn-on” strategy for rapid fluorometric detection of perfluoroctane sulfonate *Microchem. J.*, 157 (2020)

[123]. Zheng Z, Yu H, Geng W-C, Hu X-Y, Wan Y-Y, Li Z, Wang Y, Guo D-S Guanidinocalix[5]arene for sensitive fluorescence detection and magnetic removal of perfluorinated pollutants *Nat. Comm.*, 10 (2019), p. 9

[124]. Fang C, Wu J, Sobhani Z, Amin MA, Tang Y Aggregated-fluorescent detection of PFAS with a simple chip *Anal. Methods*, 11 (2019), pp. 163–170

[125]. Santra B, Shneider MN, Car R In situ Characterization of Nanoparticles Using Rayleigh Scattering *Sci. Rep.*, 7 (2017), p. 40230

[126]. Qiao M, Jiang J, Liu S, Yang J, Tan K, Zhu J, Shi Y, Hu X Triple-wavelength overlapping resonance Rayleigh scattering method for facile and rapid assay of perfluoroctane sulfonate *Environ. Monit. Assess.*, 187 (2015)

[127]. Cheng Z, Zhang F, Chen X, Du L, Gao C, Tan K Highly sensitive and selective detection of perfluoroctane sulfonate based on the Janus Green B resonance light scattering method *Anal. Methods*, 8 (2016), pp. 8042–8048

[128]. Chen Q, Cheng Z, Du L, Zhu P, Tan K A sensitive three-signal assay for the determination of PFOS based on the interaction with Nile blue A *Anal. Methods*, 10 (2018), pp. 3052–3058

[129]. Fang C, Megharaj M, Naidu R Surface-enhanced Raman scattering (SERS) detection of fluorosurfactants in firefighting foams *RSC Adv.*, 6 (2016), pp. 11140–11145

[130]. Poma A, Turner AP, Piletsky SA Advances in the manufacture of MIP nanoparticles *Trends Biotechnol.*, 28 (2010), pp. 629–637 [PubMed: 20880600]

[131]. Aragay G, Pino F, Merkoçi A Nanomaterials for Sensing and Destroying Pesticides *Chem. Rev.*, 112 (2012), pp. 5317–5338 [PubMed: 22897703]

[132]. Thatai S, Khurana P, Boken J, Prasad S, Kumar D Nanoparticles and core–shell nanocomposite based new generation water remediation materials and analytical techniques: A review *Microchem. J.*, 116 (2014), pp. 62–76

[133]. Wang C, Yu C Detection of chemical pollutants in water using gold nanoparticles as sensors: a review *Rev. Anal. Chem.*, 32 (2013), pp. 1–14

[134]. Qin L, Zeng G, Lai C, Huang D, Xu P, Zhang C, Cheng M, Liu X, Liu S, Li B, Yi H “Gold rush” in modern science: Fabrication strategies and typical advanced applications of gold nanoparticles in sensing *Coord. Chem. Rev.*, 359 (2018), pp. 1–31

[135]. Kim HN, Ren WX, Kim JS, Yoon J Fluorescent and colorimetric sensors for detection of lead, cadmium, and mercury ions *Chem. Soc. Rev.*, 41 (2012), pp. 3210–3244 [PubMed: 22184584]

[136]. Deng J, Yu P, Wang Y, Yang L, Mao L Visualization and quantification of neurochemicals with gold nanoparticles: opportunities and challenges *Adv. Mater.*, 26 (2014), pp. 6933–6943 [PubMed: 24639384]

[137]. Pezzato C, Maiti S, Chen J-Y, Cazzolaro A, Gobbo C, Prins L Monolayer protected gold nanoparticles with metal-ion binding sites: functional systems for chemosensing applications *Chem. Commun.*, 51 (2015), pp. 9922–9931

[138]. Pingarrón JM, Yanez-Sedeno P, González-Cortés A Gold nanoparticle-based electrochemical biosensors *Electrochim. Acta*, 53 (2008), pp. 5848–5866

[139]. Aragay G, Pons J, Merkoçi A Recent trends in macro-, micro-, and nanomaterial-based tools and strategies for heavy-metal detection *Chem. Rev.*, 111 (2011), pp. 3433–3458 [PubMed: 21395328]

[140]. Sabela M, Balme S, Bechelany M, Janot J-M, Bisetty K A Review of Gold and Silver Nanoparticle-Based Colorimetric Sensing Assays *Adv. Eng. Mater.*, 19 (2017), p. 24

[141]. Chang C-C, Chen C-P, Wu T-H, Yang C-H, Lin C-W, Chen C-Y Gold Nanoparticle-Based Colorimetric Strategies for Chemical and Biological Sensing Applications *Nanomaterials*, 9 (2019), p. 861 [PubMed: 31174348]

[142]. Liu J, Du J, Su Y, Zhao H A facile solvothermal synthesis of 3D magnetic MoS<sub>2</sub>/Fe<sub>3</sub>O<sub>4</sub> nanocomposites with enhanced peroxidase-mimicking activity and colorimetric detection of perfluorooctane sulfonate *Microchem. J.*, 149 (2019), Article 104019

[143]. Kairdolf BA, Smith AM, Stokes TH, Wang MD, Young AN, Nie S Semiconductor quantum dots for bioimaging and biodiagnostic applications *Annu. Rev. Anal. Chem.*, 6 (2013), pp. 143–162

[144]. Alivisatos P The use of nanocrystals in biological detection *Nat. Biotechnol.*, 22 (2004), pp. 47–52 [PubMed: 14704706]

[145]. Liu Q, Huang A, Wang N, Zheng G, Zhu L Rapid fluorometric determination of perfluorooctanoic acid by its quenching effect on the fluorescence of quantum dots *J. Lumin.*, 161 (2015), pp. 374–381

[146]. Baker SN, Baker GA Luminescent carbon nanodots: emergent nanolights *Angew. Chem. Int. Ed.*, 49 (2010), pp. 6726–6744

[147]. Li H, Kang Z, Liu Y, LeeCarbon S-T nanodots: synthesis, properties and applications *J. Mater. Chem.*, 22 (2012), pp. 24230–24253

[148]. Cheng Z, Dong H, Liang J, Zhang F, Chen X, Du L, Tan K Highly selective fluorescent visual detection of perfluorooctane sulfonate via blue fluorescent carbon dots and berberine chloride hydrate *Spectrochim. Acta, Part A*, 207 (2019), pp. 262–269

[149]. Chen Q, Zhu P, Xiong J, Gao L, Tan K A sensitive and selective triple-channel optical assay based on red-emissive carbon dots for the determination of PFOS *Microchem. J.*, 145 (2019), pp. 388–396

[150]. Sun X, Lei Y Fluorescent carbon dots and their sensing applications, *TrAC Trends Anal. Chem.*, 89 (2017), pp. 163–180

[151]. Walekar LS, Zheng M, Zheng L, Long M Selenium and nitrogen co-doped carbon quantum dots as a fluorescent probe for perfluorooctanoic acid *Microchim. Acta*, 186 (2019)

[152]. Soh JH, Chan H-M, Ying JY Strategies for developing sensitive and specific nanoparticle-based lateral flow assays as point-of-care diagnostic device *Nano Today*, 30 (2020), Article 100831

[153]. Moro G, De Wael K, Moretto LM Challenges in the electrochemical (bio)sensing of nonelectroactive food and environmental contaminants *Curr. Opin. Electrochem.*, 16 (2019), pp. 57–65

[154]. Lahcen AA, Amine A Recent advances in electrochemical sensors based on molecularly imprinted polymers and nanomaterials *Electroanalysis*, 31 (2019), pp. 188–201

[155]. Karoyo AH, Wilson LD Tunable macromolecular-based materials for the adsorption of perfluorooctanoic and octanoic acid anions *J. Colloid Interface Sci.*, 402 (2013), pp. 196–203 [PubMed: 23664395]

[156]. Fang C, Chen Z, Megharaj M, Naidu R Potentiometric detection of AFFFs based on MIP *Environ. Technol. Inno.*, 5 (2016), pp. 52–59

[157]. Chen S, Li A, Zhang L, Gong J Molecularly imprinted ultrathin graphitic carbon nitride nanosheets-Based electrochemiluminescence sensing probe for sensitive detection of perfluorooctanoic acid *Anal. Chim. Acta*, 896 (2015), pp. 68–77 [PubMed: 26481989]

[158]. Karimian N, Stortini AM, Moretto LM, Costantino C, Bogianni S, Ugo P Electrochemosensor for trace analysis of perfluorooctane sulfonate in water based on a molecularly imprinted poly o-phenylenediamine polymer *ACS Sensors*, 3 (2018), pp. 1291–1298 [PubMed: 29911865]

[159]. Kazemi R, Potts EI, Dick JE Quantifying Interferent Effects on Molecularly Imprinted Polymer Sensors for Per- and Polyfluoroalkyl Substances (PFAS) *Anal. Chem.*, 92 (2020), pp. 10597–10605 [PubMed: 32564597]

[160]. Moro G, Cristofori D, Bottari F, Cattaruzza E, De Wael K, Moretto LM Redesigning an Electrochemical MIP Sensor for PFOS: Practicalities and Pitfalls *Sensors*, 19 (2019), p. 4433 [PubMed: 31614913]

[161]. Malitestà C, Losito I, Zambonin PG Molecularly Imprinted Electrosynthesized Polymers: New Materials for Biomimetic Sensors *Anal. Chem.*, 71 (1999), pp. 1366–1370 [PubMed: 21662960]

[162]. Tran T, Li J, Feng H, Cai J, Yuan L, Wang N, Cai Q Molecularly imprinted polymer modified TiO<sub>2</sub> nanotube arrays for photoelectrochemical determination of perfluorooctane sulfonate (PFOS) *Sens. Actuators B Chem.*, 190 (2014), pp. 745–751

[163]. Gong J, Fang T, Peng D, Li A, Zhang L A highly sensitive photoelectrochemical detection of perfluorooctanoic acid with molecularly imprinted polymer-functionalized nanoarchitectured hybrid of AgI–BiOI composite *Biosens. Bioelectron.*, 73 (2015), pp. 256–263 [PubMed: 26092130]

[164]. Roy P, Berger S, Schmuki P TiO<sub>2</sub> nanotubes: synthesis and applications *Angew. Chem. Int. Ed.*, 50 (2011), pp. 2904–2939

[165]. Zlamal M, Macak JM, Schmuki P, Krýsa J Electrochemically assisted photocatalysis on self-organized TiO<sub>2</sub> nanotubes *Electrochem. Commun.*, 9 (2007), pp. 2822–2826

[166]. Tokonami S, Shiigi H, Nagaoka Review T: Micro- and nanosized molecularly imprinted polymers for high-throughput analytical applications *Anal. Chim. Acta*, 641 (2009), pp. 7–13

[167]. Feng H, Wang N, Tran T, Yuan L, Li J, Cai Q Surface molecular imprinting on dye–(NH<sub>2</sub>)-SiO<sub>2</sub> NPs for specific recognition and direct fluorescent quantification of perfluorooctane sulfonate *Sens. Actuators B Chem.*, 195 (2014), pp. 266–273

[168]. Zheng L, Zheng Y, Liu Y, Long S, Du L, Liang J, Huang C, Swihart MT, Tan K Core-shell quantum dots coated with molecularly imprinted polymer for selective photoluminescence sensing of perfluorooctanoic acid *Talanta*, 194 (2019), pp. 1–6 [PubMed: 30609506]

[169]. Jiao Z, Li J, Mo L, Liang J, Fan H A molecularly imprinted chitosan doped with carbon quantum dots for fluorometric determination of perfluorooctane sulfonate *Microchim. Acta*, 185 (2018)

[170]. Cahoon LB, GenX Contamination of the Cape Fear River, North Carolina: Analytical Environmental Chemistry Uncovers Multiple System Failures, Elsevier 2019, pp. 341–354.

[171]. Lorenzo R, Carro A, Alvarez-Lorenzo C, Concheiro A To Remove or Not to Remove? The Challenge of Extracting the Template to Make the Cavities Available in Molecularly Imprinted Polymers (MIPs) *Int. J. Mol. Sci.*, 12 (2011), pp. 4327–4347 [PubMed: 21845081]

[172]. Glasscott MW, Vannoy KJ, Kazemi R, Verber MD, Dick JE μ-MIP: Molecularly Imprinted Polymer-Modified Microelectrodes for the Ultrasensitive Quantification of GenX (HFPO-DA) in River Water *Environ. Sci. Technol. Lett.*, 7 (2020), pp. 489–495

[173]. Cennamo N, Arcadio F, Capasso F, Perri C, D'Agostino G, Porto G, Biasiolo A, Zeni L Towards Smart Selective Sensors exploiting a novel approach to connect Optical Fiber Biosensors in Internet *IEEE Trans. Instrum. Meas.*, 1–1 (2020)

[174]. Cennamo N, Arcadio F, Perri C, Zeni L, Sequeira F, Bilro L, Nogueira R, D'Agostino G, Porto G, Biasiolo A Water monitoring in smart cities exploiting plastic optical fibers and molecularly imprinted polymers The case of PFBS detection, 2019 IEEE International Symposium on Measurements & Networking (M&N) (2019), pp. 1–6

[175]. Liu T, Wang W, Jian D, Li J, Ding H, Yi D, Liu F, Wang S Quantitative remote and on-site Hg<sup>2+</sup> detection using the handheld smartphone based optical fiber fluorescence sensor (SOFSS) *Sens. Actuators B Chem.*, 301 (2019), Article 127168

[176]. Cennamo N, Massarotti D, Conte L, Zeni L Low Cost Sensors Based on SPR in a Plastic Optical Fiber for Biosensor Implementation *Sensors*, 11 (2011), pp. 11752–11760 [PubMed: 22247691]

[177]. Cennamo N, Zeni L, Tortora P, Regonesi ME, Giusti A, Staiano M, D'Auria S, Varriale A A high sensitivity biosensor to detect the presence of perfluorinated compounds in environment *Talanta*, 178 (2018), pp. 955–961 [PubMed: 29136923]

[178]. Sharma AK, Pandey AK, Kaur B A Review of advancements (2007–2017) in plasmonics-based optical fiber sensors *Opt. Fiber Technol.*, 43 (2018), pp. 20–34

[179]. Gupta BD, Verma RK Surface Plasmon Resonance-Based Fiber Optic Sensors: Principle, Probe Designs, and Some Applications *J. Sens.*, 2009 (2009), pp. 1–12

[180]. Cennamo N, Zeni L Polymer Optical Fibers for Sensing *Macromol. Symp.*, 389 (2020), p. 1900074

[181]. Cennamo N, Massarotti D, Galatus R, Conte L, Zeni L Performance Comparison of Two Sensors Based on Surface Plasmon Resonance in a Plastic Optical Fiber Sensors, 13 (2013), pp. 721–735 [PubMed: 23296329]

[182]. Cennamo N, D'Agostino G, Porto G, Biasiolo A, Perri C, Arcadio F, Zeni L A Molecularly Imprinted Polymer on a Plasmonic Plastic Optical Fiber to Detect Perfluorinated Compounds in Water Sensors, 18 (2018), p. 1836 [PubMed: 29874860]

[183]. Cennamo N, D'Agostino G, Sequeira F, Mattiello F, Porto G, Biasiolo A, Nogueira R, Bilro L, Zeni L A Simple and Low-Cost Optical Fiber Intensity-Based Configuration for Perfluorinated Compounds in Water Solution Sensors, 18 (2018), p. 3009 [PubMed: 30205565]

[184]. Cennamo N, Zeni L, D'Agostino G, Porto G, Biasiolo A Optical chemical fiber sensor for the detection of perfluorinated compounds in water Institute of Electrical and Electronics Engineers (2018)

[185]. Faiz F, Baxter G, Collins S, Sidioglou F, Cran M Polyvinylidene fluoride coated optical fibre for detecting perfluorinated chemicals *Sens. Actuators B Chem*, 312 (2020), Article 128006

[186]. Chen H, He P, Rao H, Wang F, Liu H, Yao J Systematic investigation of the toxic mechanism of PFOA and PFOS on bovine serum albumin by spectroscopic and molecular modeling *Chemosphere*, 129 (2015), pp. 217–224 [PubMed: 25497588]

[187]. Liu X, Fang M, Xu F, Chen D Characterization of the binding of per- and poly-fluorinated substances to proteins: A methodological review, *TrAC Trends Anal. Chem*, 116 (2019), pp. 177–185

[188]. Wang Y, Zhang H, Kang Y, Cao J Effects of perfluorooctane sulfonate on the conformation and activity of bovine serum albumin *J. Photochem. Photobiol., B*, 159 (2016), pp. 66–73 [PubMed: 27031195]

[189]. Zhang X, Chen L, Fei X-C, Ma Y-S, Gao H-W Binding of PFOS to serum albumin and DNA: insight into the molecular toxicity of perfluorochemicals *BMC Mol. Biol*, 10 (2009), p. 16 [PubMed: 19239717]

[190]. Moro G, Bottari F, Liberi S, Covaceuszach S, Cassetta A, Angelini A, De Wael K, Moretto LM Covalent immobilization of delipidated human serum albumin on poly (pyrrole-2-carboxylic acid film for the impedimetric detection of perfluorooctanoic acid *Bioelectrochemistry*, 134 (2020), Article 107540

[191]. Xia W, Wan Y-J, Wang X, Li Y-Y, Yang W-J, Wang C-X, Xu S-Q Sensitive bioassay for detection of PPAR $\alpha$  potentially hazardous ligands with gold nanoparticle probe *J. Hazard. Mater*, 192 (2011), pp. 1148–1154 [PubMed: 21726938]

[192]. Zhang J, Wan Y, Li Y, Zhang Q, Xu S, Zhu H, Shu B A rapid and high-throughput quantum dots bioassay for monitoring of perfluorooctane sulfonate in environmental water samples *Environ. Pollut*, 159 (2011), pp. 1348–1353 [PubMed: 21345559]

[193]. Zhang T, Zhao H, Lei A, Quan X Electrochemical Biosensor for Detection of Perfluorooctane Sulfonate Based on Inhibition Biocatalysis of Enzymatic Fuel Cell *Electrochemistry*, 82 (2014), pp. 94–99

[194]. Rogge SMJ, Bavykina A, Hajek J, Garcia H, Olivos-Suarez AI, Sepúlveda-Escribano A, Vimont A, Clet G, Bazin P, Kapteijn F, Daturi M, Ramos-Fernandez EV, Llabrés FX, Xamena I, Van Speybroeck V, Gascon J Metal–organic and covalent organic frameworks as single-site catalysts *Chem. Soc. Rev*, 46 (2017), pp. 3134–3184 [PubMed: 28338128]

[195]. Cheng YH, Barpaga D, Soltis JA, Shutthanandan V, Kargupta R, Han KS, McGrail BP, Motkuri RK, Basuray S, Chatterjee S Metal–Organic Framework-Based Microfluidic Impedance Sensor Platform for Ultrasensitive Detection of Perfluorooctanesulfonate *ACS Appl. Mater. Sci.*, 12 (2020), pp. 10503–10514

[196]. Diercks CS, Yaghi OM The atom, the molecule, and the covalent organic framework *Science*, 355 (2017), pp. 923–933

[197]. Li J, Zhang C, Yin M, Zhang Z, Chen Y, Deng Q, Wang S Surfactant-Sensitized Covalent Organic Frameworks-Functionalized Lanthanide-Doped Nanocrystals: An Ultrasensitive Sensing Platform for Perfluorooctane Sulfonate *ACS Omega*, 4 (2019), pp. 15947–15955 [PubMed: 31592465]

[198]. Chen LD, Lai C-Z, Granda LP, Fierke MA, Mandal D, Stein A, Gladysz JA, Bühlmann P Fluorous Membrane Ion-Selective Electrodes for Perfluorinated Surfactants: Trace-Level Detection and in Situ Monitoring of Adsorption Anal. Chem, 85 (2013), pp. 7471–7477 [PubMed: 23789785]

[199]. Chen LD, Mandal D, Gladysz JA, Bühlmann P Chemical stability and application of a fluorophilic tetraalkylphosphonium salt in fluorous membrane anion-selective electrodes New J. Chem, 34 (2010), p. 1867

[200]. Ugo P, Karimian N, Stortini AM, Moretto LM New molecularly-imprinted electrochemical sensors for perfluoroctansulfonate and analytical methods based thereon Foscari University of Venice, Ca' (2017)

[201]. Motkuri RK, Chatterjee S, Barpaga D, Mcgrail BP, Composition and method for capture and degradation of PFAS, Battelle Memorial Institute Inc., 2020.

[202]. Regulation (EU) 2019/1021 of the European Parliament and of the Council of 20 June 2019 on persistent organic pollutants, 2019.

[203]. Kucharzyk KH, Darlington R, Benotti M, Deeb R, Hawley E Novel treatment technologies for PFAS compounds: A critical review J. Environ. Manage, 204 (2017), pp. 757–764 [PubMed: 28818342]

[204]. Kumarasamy E, Manning IM, Collins LB, Coronell O, Leibfarth FA Ionic Fluorogels for Remediation of Per- and Polyfluorinated Alkyl Substances from Water ACS Cent. Sci, 6 (2020), pp. 487–492 [PubMed: 32341998]

[205]. Takezawa H, Murase T, Resnati G, Metrangolo P, Fujita M Recognition of Polyfluorinated Compounds Through Self-Aggregation in a Cavity J. Am. Chem. Soc, 136 (2014), pp. 1786–1788 [PubMed: 24422785]

[206]. Karoyo A, Wilson L Nano-Sized Cyclodextrin-Based Molecularly Imprinted Polymer Adsorbents for Perfluorinated Compounds—A Mini-Review Nanomaterials, 5 (2015), pp. 981–1003 [PubMed: 28347047]

[207]. Weiss-Errico MJ, O'Shea KE Enhanced host–guest complexation of short chain perfluoroalkyl substances with positively charged  $\beta$ -cyclodextrin derivatives J. Incl. Phenom. Macro, 95 (2019), pp. 111–117

[208]. Yang A, Ching C, Easler M, Helbling DE, Dichtel W Cyclodextrin Polymers with Nitrogen-Containing Tripodal Crosslinkers for Efficient PFAS Adsorption ACS Mater. Lett, 2 (2020), pp. 1240–1245

[209]. Guo H, Liu Y, Ma W, Yan L, Li K, Lin S Surface molecular imprinting on carbon microspheres for fast and selective adsorption of perfluoroctane sulfonate J. Hazard. Mater, 348 (2018), pp. 29–38 [PubMed: 29367130]

[210]. Du L, Cheng Z, Zhu P, Chen Q, Wu Y, Tan K Preparation of mesoporous silica nanoparticles molecularly imprinted polymer for efficient separation and enrichment of perfluoroctane sulfonate J. Sep. Sci, 41 (2018), pp. 4363–4369 [PubMed: 30298988]

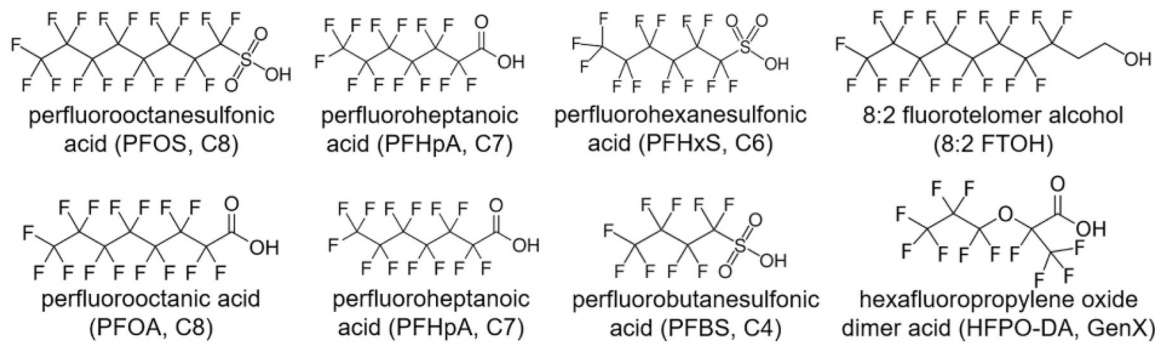
[211]. Du L, Wu Y, Zhang X, Zhang F, Chen X, Cheng Z, Wu F, Tan K Preparation of magnetic molecularly imprinted polymers for the rapid and selective separation and enrichment of perfluoroctane sulfonate J. Sep. Sci, 40 (2017), pp. 2683–2848

[212]. Cao F, Wang L, Tian Y, Wu F, Deng C, Guo Q, Sun H, Lu S Synthesis and evaluation of molecularly imprinted polymers with binary functional monomers for the selective removal of perfluoroctanesulfonic acid and perfluoroctanoic acid J. Chromatogr. A, 1516 (2017), pp. 42–53 [PubMed: 28823786]

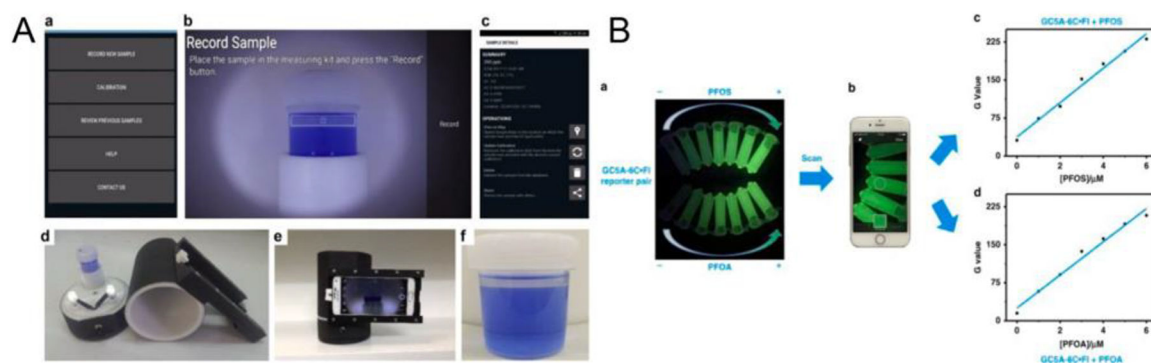
[213]. Mohd Azmi LH, Williams D, Ladewig BP Polymer-assisted modification of metal-organic framework MIL-96 (Al): influence of HPAM concentration on particle size, crystal morphology and removal of harmful environmental pollutant PFOA Chemosphere, 262 (2020), Article 128072

**Highlights**

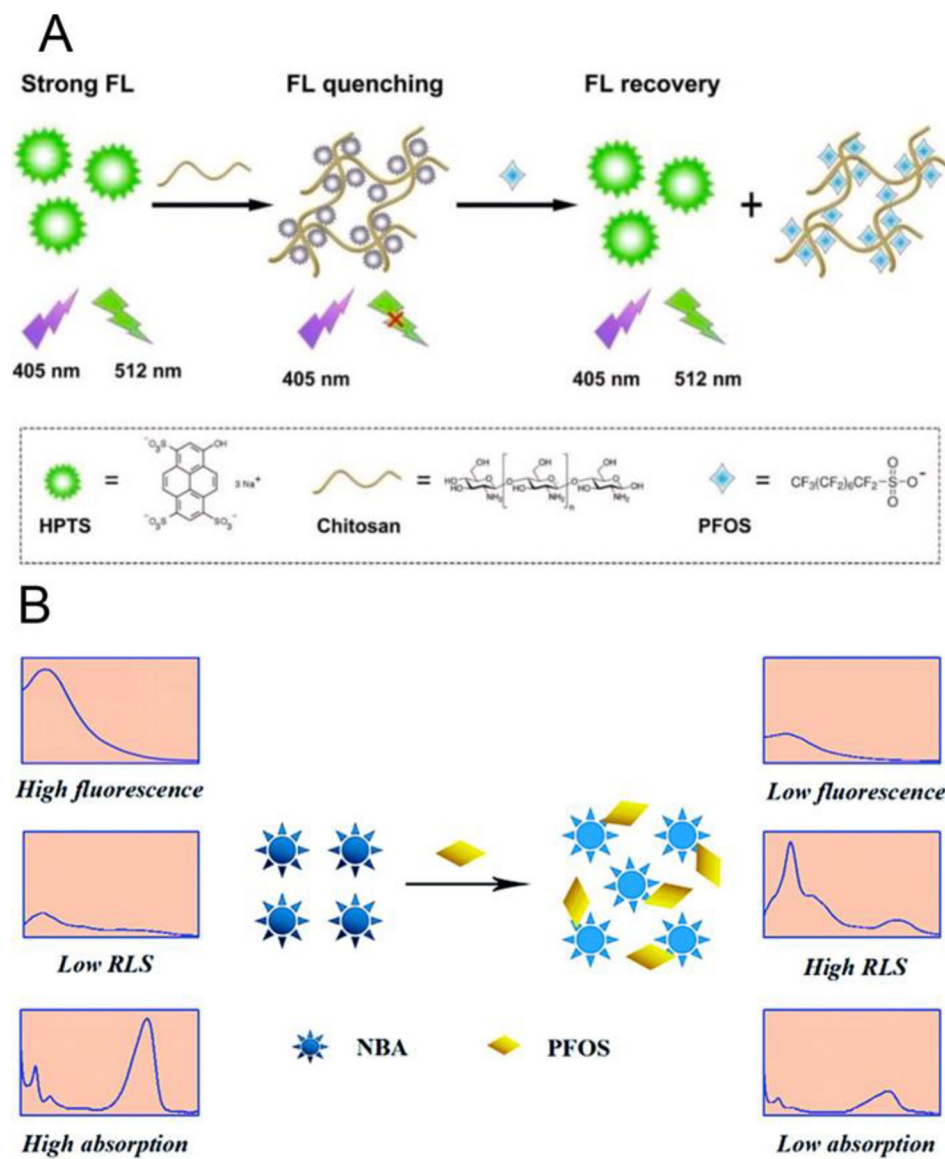
- Review of PFAS sensors focusing on key molecular mechanisms.
- Sensors to detect PFAS are needed as an alternative to traditional instrumentation.
- MIPs and immunoassays have the lowest PFAS detection limits.
- High detection limits currently hamper PFAS sensor commercialization.



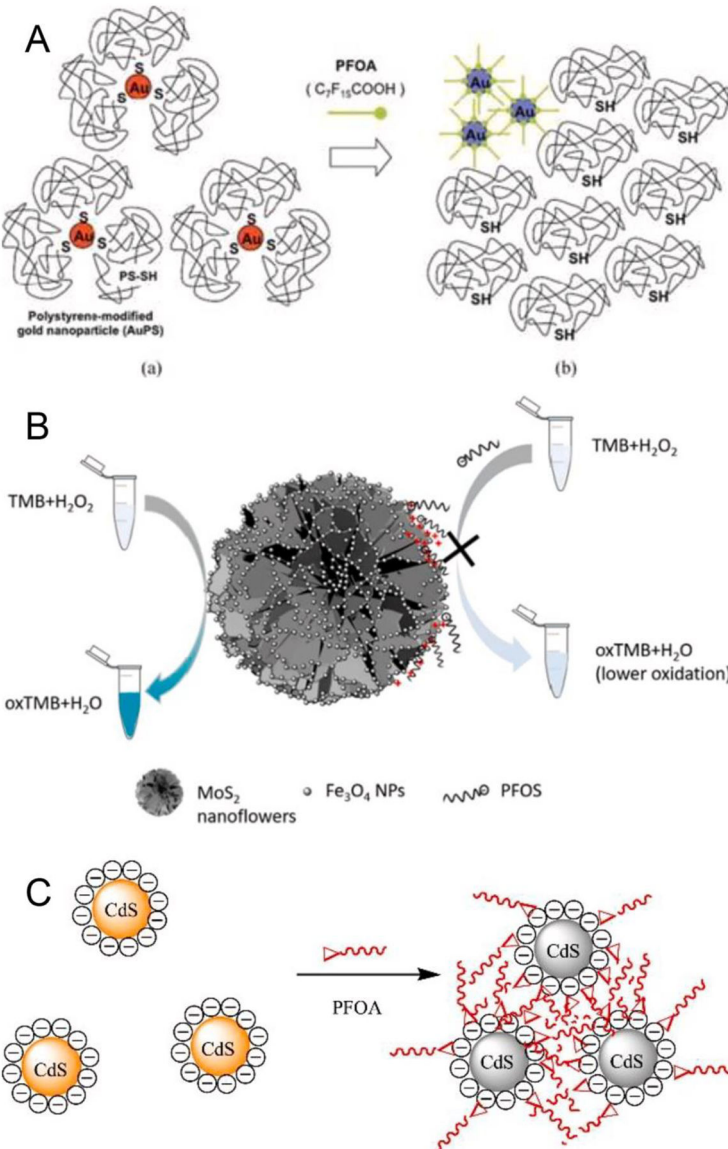
**Fig. 1.**  
Example of common per and poly-fluoroalkyl substances (PFAS).

**Fig. 2.**

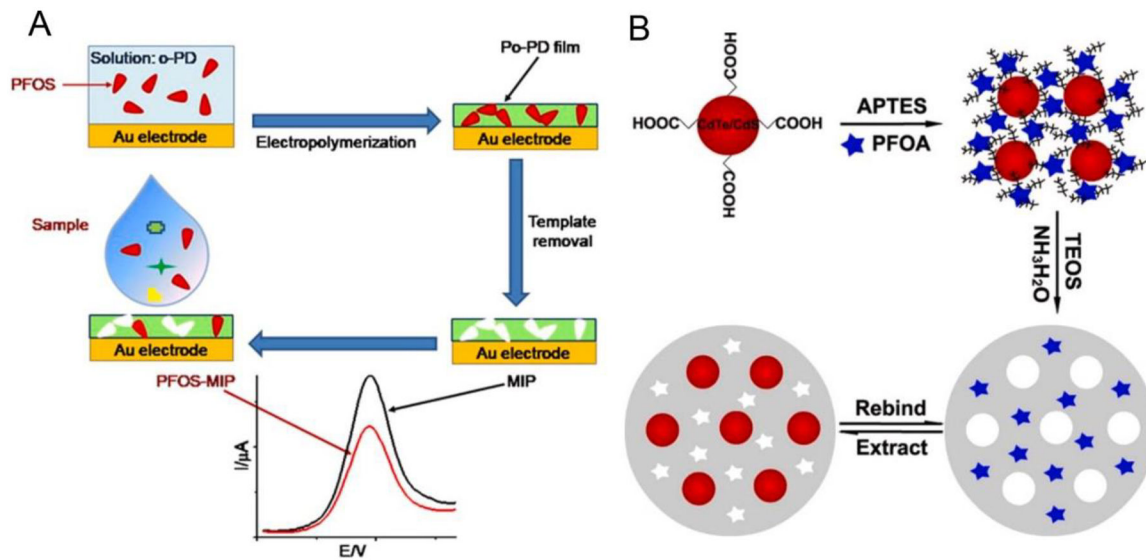
A. Demonstration of astkCARE kit to analyze PFOS by reading the blue color with a smartphone. Reprinted with permission from Fang et al., 2018. B. A smartphone is used to detect the change in fluorescence due to the complexation of PFOS and PFOA with guanidinocalix[5]arene. Reprinted with permission from Zheng et al., 2019.

**Fig. 3.**

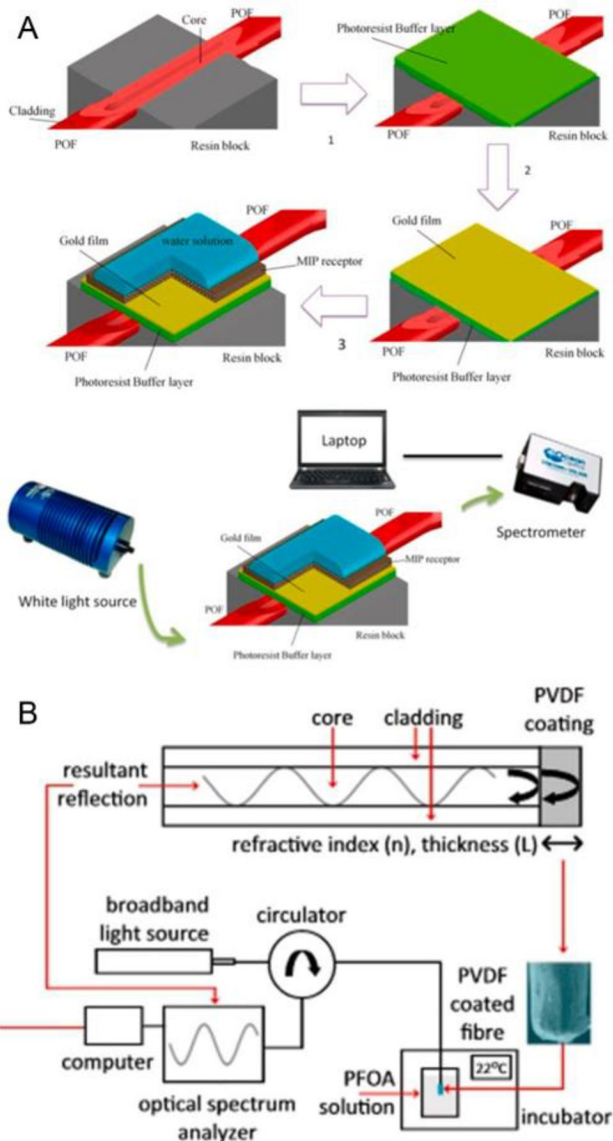
A. A schematic of a chitosan-mediated fluorescence “turn-on” method for PFOS detection. Reprinted with permission from He et al., 2020. B. A schematic of a three-signal assay for PFOS detection in aqueous solution based on fluorescence, absorption and resonance light scattering (RLS). Reprinted with permission from Chen et al., 2018.

**Fig. 4.**

A. PFOA detection using polystyrene-modified **gold nanoparticles**. Reprinted with permission from Takayose et al., 2012. B. A schematic of colorimetric PFOS detection by peroxidase-mimicking 3D magnetic  $MoS_2/Fe_3O_4$  nanocomposites. Reprinted with permission from Liu et al., 2019. C. Fluorescent detection of PFOA by the aggregation of MPA-CdS quantum dots. Reprinted with permission from Liu et al., 2015.

**Fig. 5.**

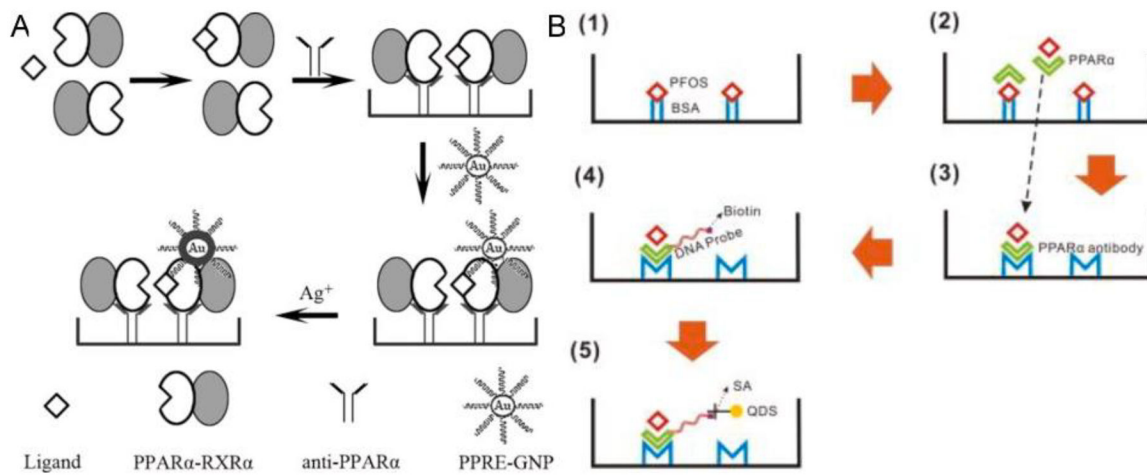
A. A schematic demonstrating the fabrication of a molecularly imprinted polymer (MIP) to detect PFOS. The MIP was fabricated by the [electropolymerization](#) of o-phenylenediamine on a gold electrode. Reprinted with permission from Karimian et al., 2018. B. Preparation of a MIP on a quantum dot with 3-aminopropyltriethoxysilane (APTES) as the functional [monomer](#) and tetraethoxysilane (TEOS) as the cross-linker in the presence of aqueous ammonia. Reprinted with permission from Zheng et al., 2019.

**Fig. 6.**

A. Steps to produce a [surface plasmon resonance](#) (SPR) sensor on a D-shaped plastic optical fiber with a MIP receptor. Reprinted with permission from Cennamo et al., 2018.

B. Schematic of a [polyvinylidene](#) fluoride-coated optical fiber for detection of PFOA.

Reprinted with permission from Faiz et al., 2020.

**Fig. 7.**

A. A schematic of PFOS detection by the silver-enhanced interaction between PPRE-modified gold nanoparticle probes and activated PPAR $\alpha$ . PPRE-GNP: PPAR $\alpha$ -responsive element-modified gold nanoparticle probes. Reprinted with permission from Xia et al., 2011.

B. Schematic of a bioassay using streptavidin–biotin-modified quantum dots to detect PFOS. Reprinted with permission from Zhang et al., 2011.

**Table 1**

Small molecule-based detection of PFAS.

Complexing agent	Analyte	LOD (ppb)	Concentration Range (ppb)	Real Sample	Detector	Detection	Ref.
Imidazolium group + MB <sup>a</sup>	Anionic surfactants	1000	NR <sup>b</sup>	Urban wastewater	Spectrometer	Absorption	[109]
MB or ethyl violet	PFOA	50	NR	Groundwater	Confocal Raman microscope	Raman	[129]
AIEgen	PFOA	41	41 – 41,000	None tested	Fluorescence spectrophotometer	Fluorescence	[124]
Guanidinocalix[5] arene	PFOS, PFOA	PFOS: 10.7 PFOA: 10.9	PFOS: 0 – 3001, PFOA: 0 – 2484	Tap and lake water	Fluorescence spectrophotometer, smartphone	Fluorescence	[123]
Ethyl violet	PFOS, PFOA	10, 0.5 with SPE <sup>c</sup>	10 – 1000	Tap and groundwater	Smartphone	Colorimetric	[112]
Eosin Y	PFOS	7.5	0 – 1000	Tap and river water	Spectrofluorometer	Fluorescence	[120]
Erythrosin B	PFOS, PFOA	PFOS: 6.4	PFOS: 25 – 5001,	Tap and river water	Spectrofluorometer	Fluorescence	[121]
Crystal violet	PFOA	PFOA: 4.9 4.6	PFOA: 21 – 4141 41 – 10,352	Tap and river water	Fluorescence spectrophotometer	RLS <sup>d</sup>	[90]
Crystal violet	PFOS	3.0	300 – 5000	Tap and river water	Fluorescence spectrophotometer	TWO-RSS <sup>e</sup>	[126]
Janus Green B	PFOS	2.8	25 – 4501	Tap and river water	Fluorescence spectrophotometer	RLS	[127]
Nile Blue A	PFOS	RLS: 59.8 Abs: <sup>f</sup> 7.4 Fluor: <sup>g</sup> 1.6	RLS: 100 – 6002, ABS: 200 – 2001, Fluor: 25 – 2001	Tap and river water	Fluorescence spectrophotometer	RLS, Absorption, Fluorescence	[128]
HPTS <sup>h</sup>	PFOS	0.5	2.5 – 1001	River and lake water	Fluorescence spectrophotometer	Fluorescence	[122]

<sup>a</sup>MB: methylene blue,<sup>b</sup>NR: not reported,<sup>c</sup>SPE: solid-phase extraction,<sup>d</sup>RLS: resonance light scattering,<sup>e</sup>TWO-RSS: triple-wavelength overlapping resonance Rayleigh scattering,<sup>f</sup>Abs: absorption,<sup>g</sup>Fluor: fluorescence,<sup>h</sup>HPTS: trisodium-8-hydroxypyrene-1, 3, 28 6-trisulfonate

**Table 2**

Nanoparticle-based PFAS detection.

Mechanism	NP <sup>a</sup> Modification	Analyte	LOD (ppb)	Concentration Range (ppb)	Real Samples	Detector	Detection	Ref.	
AuNP	Polystyrene	PFOA	103517 <sup>*</sup>	NR <sup>b</sup>	None tested	Photodiode array spectrophotometer	Colorimetric	[84]	
Carbon dot (CD)	Se and N doped	PFOA	745.2	4141 – 28,985	Tap and lake water	Fluorescence spectrophotometer	Fluorescence	[151]	
Quantum dot (QD)	MPA <sup>c</sup> -CdS QD	PFOA	124.2	207 – 16,563	Textile	Spectrofluorometer	Fluorescence	[145]	
Carbon dot	NA	PFOS	Fluor: <sup>d</sup> 9.13, Abs: <sup>e</sup> 37.9, RLS: <sup>f</sup> 60.2	Fluor: 100 – 6002, Abs: 250 – 4001, RLS: 250 – 6002	Tap and river water	Fluorescence spectrophotometer	Fluorescence, Absorption, RLS	[149]	
Carbon dot	N-doped with Victoria blue b	PFOS	13.9	0 – 1000	Tap and river water	Fluorescence spectrophotometer	Fluorescence	[91]	
Carbon dot	NA	PFOS	10.8	110 – 25,006	Tap and river water	Fluorescence spectrophotometer	Fluorescence	[148]	
AuNP	PEG <sup>g</sup> -thiol and perfluorinated thiol terminated	CF <sub>2</sub>	7	10	0.1 – 1000	Tap and river water	Spectrometer	Absorption	[89]
Fe <sub>3</sub> O <sub>4</sub> NP	Fe <sub>3</sub> O <sub>4</sub> NPs on MoS <sub>2</sub>	PFOS	4.3	50 – 6251	None tested	Microplate Reader	Absorption	[142]	

<sup>\*</sup> Not a true LOD, analyte concentrations as low as the given value could be clearly detected.

<sup>a</sup> NP: nanoparticle,

<sup>b</sup> NR, not reported,

<sup>c</sup> MPA: mercaptopropionic acid,

<sup>d</sup> Fluor: fluorescence,

<sup>e</sup> Abs: absorption,

<sup>f</sup> RLS: resonance light scattering,

<sup>g</sup> PEG: poly(ethylene glycol)

**Table 3**

Molecularly imprinted polymer (MIP) - based PFAS detection methods.

Substrate	MIP Template	Analytics	LOD (ppb)	Concentration Range (ppb)	Real Samples	Detection	Probe	Ref.
Gold screen-printed electrode	o-PD <sup>a</sup>	PFOS	NR <sup>b</sup>	NR	None tested	Electrochemistry: DPV <sup>c</sup>	FcCOOH	[160]
TiO <sub>2</sub> nanotube array	Acrylamide, EGDMA, AIBN <sup>d</sup>	PFOS	86	250 – 5001	Tap, river, and mountain water	Photoelectrochemistry	NA	[162]
Pencil lead	Polypyrrole	PFOA	41	4141 – 4,140,700	None tested	Electrochemistry: Potentiometry	NA	[156]
CdTe@CdS quantum dot	APTES, TEOS <sup>e</sup>	PFOA	10.4	104 – 6211	Tap and river water	Photoluminescence	NA	[168]
AgI nanoparticle-BiOI nanoflake array	Acrylamide, EGDMA, AIBN	PFOA	0.01	0.02 – 1000	Tap and river water	Photoelectrochemistry	TEA <sup>f</sup>	[163]
SiO <sub>2</sub> NP	Fluorescence dye and organic amine	PFOS	5.57	5.57 – 48.54	Surface river water	Fluorescence	NA	[167]
“Classic” flat gold electrode	o-PD	PFOS	0.02	0.05 – 2.45, 4.75 – 750	Distilled, tap, bottled mineral water	Electrochemistry: DPV	FcCOOH	[158]
Ultrathin g-C <sub>3</sub> N <sub>4</sub> nanosheet	Polypyrrole	PFOA	4.001	0.02 – 40, 50 – 400	Tap, river, and lake water	Electrochemiluminescence	SO <sup>–</sup>	[157]
Gold microelectrode	o-PD	GenX (HFPO-DA)	0.086 ppt	0.35 – 1735 ppt	River water	Electrochemistry: DPV	FcMeOH	[172]
Carbon dot	Chitosan	PFOS	0.0004 ppt	0.02 – 0.2 ppt	Serum and urine	Fluorescence	NA	[169]

<sup>a</sup> o-PD: o-phenylenediamine,<sup>b</sup> NR: not reported,<sup>c</sup> DPV: differential pulse voltammetry,<sup>d</sup> acrylamide (functional monomer), EGDMA: ethylene glycol dimethyl- lacrylate (crosslinker), AIBN: azobisisobutyronitrile (initiator agent),<sup>e</sup> APTES: 3-aminopropyltriethoxysilane (functional monomer), TEOS: tetraethoxysilane (cross-linker),<sup>f</sup> TEA: triethanolamine,<sup>g</sup> HFPO-DA: hexafluoropropylene oxide-dimer acid

**Table 4.**

Optical fiber-based sensors.

Mechanism	Analyte	LOD (ppb)	Concentration Range (ppb)	Detector	Measurement	Template	Substrate	Ref.
OF <sup>a</sup>	PFOA	~5000	0 – 60,000	Optical spectrum analyzer	Optical path difference	PVDF <sup>b</sup> with Butvar as crosslinker	End-face of freshly cleaved glass OF	[185]
OF – MIP <sup>c</sup>	PFOA	0.5	0 – 200	LED, 2 photodetectors	Resonance wavelength	VBT and PFDA, EDMA, AIBN <sup>d</sup>	D-shaped POF <sup>e</sup> with optical buffer layer + gold film	[183]
OF - Immunoassay	PFOA	0.24	0 – 100	Halogen light, spectrometer	Resonance wavelength	Anti-PFOA antibody	D-shaped POF with optical buffer layer + gold film	[177]
OF - MIP	PFOA	0.21	0 – 100	Halogen light, spectrometer	Resonance wavelength	VBT and PFDA, EDMA, AIBN	D-shaped POF with optical buffer layer + gold film	[184]
OF - MIP	C4-C11 PFAS mixture	0.15	0 – 10	Halogen light, spectrometer	Resonance wavelength	VBT and PFDA, EDMA, AIBN	D-shaped POF with optical buffer layer + gold film	[182]
OF - MIP	PFOA	0.13	0 – 4	Halogen light, spectrometer	Resonance wavelength	VBT and PFDA, EDMA, AIBN	D-shaped POF with optical buffer layer + gold film	[182]
OF - MIP	PFBS	< 1	0 – 21	LED, Arduino, Raspberry Pi	Resonance wavelength	VBT and PFDA, EDMA, AIBN	D-shaped POF with optical buffer layer + gold film	[174]

<sup>a</sup> OF: optical fiber,<sup>b</sup> PVDF: polyvinylidene fluoride,<sup>c</sup> MIP: molecularly imprinted polymer,<sup>d</sup> VBT: (vinylbenzyl)trimethylammonium chloride and PFDA: 1H,1H,2H,2H-perfluorodecyl acrylate (functional monomers), EGDMA: ethylene glycol dimethylacrylate (crosslinker), AIBN: azobisisobutyronitrile (radical initiator),<sup>e</sup> POF: plasmonic optical fiber.

**Table 5**

Immunosensors.

Substrate	Mechanism	Analytes	LOD (ppb)	Concentration Range (ppb)	Real Samples	Detector	Measurement	Ref.
Graphite screen-printed electrode	PFOA binds to human serum albumin	PFOA	207	207 – 828	None tested	Potentiostat/galvanostat	Electrochemistry: impedance	[190]
Multi-walled carbon nanohorn-modified glassy carbon electrode	PFOS inhibits catalysis of glutamic dehydrogenase and bilirubin oxidase	PFOS	0.80	2.50 – 250	Reservoir and river water	Potentiostat	Electrochemistry: cyclic voltammetry	[193]
Gold nanoparticle	PPRE <sup>a</sup> -modified AuNP bind to PFOS-activated PPAR $\alpha$ complex	PFOS	0.005	0.05 – 500	River water	Microplate reader	Optical density	[191]
Quantum dot (QD)	Streptavidin QDs bind to PFOS-activated PPAR $\alpha$ complex	PFOS	0.0025	0.0025 – 0.075	River, lake, bottled purified water	Microplate reader	Fluorescence	[192]

<sup>a</sup>PPRE: PPAR (peroxisome proliferator-activated receptor) response element.